Accelerated Article Preview

Rapid epidemic expansion of the SARS-CoV-2 Omicron variant in southern Africa

Raquel Viana, Sikhulile Moyo, Daniel G. Amoako, Houriiyah Tegally, Cathrine Scheepers, Christian L. Althaus, Ugochukwu J. Anyaneji, Phillip A. Bester, Maciej F. Boni, Mohammed Chand, Wonderful T. Choga, Rachel Colquhoun, Michaela Davids, Koen Deforche, Deelan Doolabh, Louis du Plessis, Susan Engelbrecht, Josie Everatt, Jennifer Giandhari, Marta Giovanetti, Diana Hardie, Verity Hill, Nei-Yuan Hsiao, Arash Iranzadeh, Arshad Ismail, Charity Joseph, Rageema Joseph, Legodile Koopile, Sergei L. Kosakovsky Pond, Moritz U. G. Kraemer, Lesego Kuate-Lere, Oluwakemi Laguda-Akingba, Onalethatha Lesetedi-Mafoko, Richard J. Lessells, Shahin Lockman, Alexander G. Lucaci, Arisha Maharaj, Boitshoko Mahlangu, Tongai Maponga, Kamela Mahlakwane, Zinhle Makatini, Gert Marais, Dorcas Maruapula, Kereng Masupu, Mogomotsi Matshaba, Simnikiwe Mayaphi, Nokuzola Mbhele, Mpaphi B. Mbulawa, Adriano Mendes, Koleka Mlisana, Anele Mnguni, Thabo Mohale, Monika Moir, Kgomotso Moruisi, Mosepele Mosepele, Gerald Motsatsi, Modisa S. Motswaledi, Thongbotho Mphoyakgosi, Nokukhanya Msomi, Peter N. Mwangi, Yeshnee Naidoo, Noxolo Ntuli, Martin Nyaga, Lucier Olubayo, Sureshnee Pillay, Botshelo Radibe, Yajna Ramphal, Upasana Ramphal, James E. San, Lesley Scott, Roger Shapiro, Lavanya Singh, Pamela Smith-Lawrence, Wendy Stevens, Amy Strydom, Kathleen Subramoney, Naume Tebeila, Derek Tshiabuila, Joseph Tsui, Stephanie van Wyk, Steven Weaver, Constantinos K. Wibmer, Eduan Wilkinson, Nicole Wolter, Alexander E. Zarebski, Boitumelo Zuze, Dominique Goedhals, Wolfgang Preiser, Florette Treurnicht, Marietje Venter, Carolyn Williamson, Oliver G. Pybus, Jinal Bhiman, Allison Glass, Darren P. Martin, Andrew Rambaut, Simani Gaseitsiwe, Anne von Gottberg & Tulio de Oliveira

Article

Rapid epidemic expansion of the SARS-CoV-2 Omicron variant in southern Africa

Raquel Viana[1,50], Sikhulile Moyo[2,3,4,50], Daniel G. Amoako[5,50], Houriiyah Tegally[6,50], Cathrine Scheepers[5,7,50], Christian L. Althaus[8], Ugochukwu J. Anyaneji[6], Phillip A. Bester[9,10], Maciej F. Boni[11], Mohammed Chand[12], Wonderful T. Choga[3], Rachel Colquhoun[13], Michaela Davids[14], Koen Deforche[15], Deelan Doolabh[16], Louis du Plessis[17,18], Susan Engelbrecht[19], Josie Everatt[5], Jennifer Giandhari[6], Marta Giovanetti[20,21], Diana Hardie[16,22], Verity Hill[13], Nei-Yuan Hsiao[16,22,23], Arash Iranzadeh[24], Arshad Ismail[5], Charity Joseph[12], Rageema Joseph[16], Legodile Koopile[2], Sergei L. Kosakovsky Pond[25], Moritz U. G. Kraemer[17], Lesego Kuate-Lere[26], Oluwakemi Laguda-Akingba[27,28], Onalethatha Lesetedi-Mafoko[29], Richard J. Lessells[6], Shahin Lockman[2,30], Alexander G. Lucaci[25], Arisha Maharaj[6], Boitshoko Mahlangu[5], Tongai Maponga[19], Kamela Mahlakwane[19,31], Zinhle Makatini[32], Gert Marais[16,22], Dorcas Maruapula[2], Kereng Masupu[4], Mogomotsi Matshaba[4,33,34], Simnikiwe Mayaphi[35], Nokuzola Mbhele[16], Mpaphi B. Mbulawa[36], Adriano Mendes[14], Koleka Mlisana[37,38], Anele Mnguni[5], Thabo Mohale[5], Monika Moir[39], Kgomotso Moruisi[26], Mosepele Mosepele[4,40], Gerald Motsatsi[5], Modisa S. Motswaledi[4,41], Thongbotho Mphoyakgosi[36], Nokukhanya Msomi[42], Peter N. Mwangi[10,43], Yeshnee Naidoo[6], Noxolo Ntuli[5], Martin Nyaga[10,43], Lucier Olubayo[23,24], Sureshnee Pillay[6], Botshelo Radibe[2], Yajna Ramphal[6], Upasana Ramphal[6], James E. San[6], Lesley Scott[44], Roger Shapiro[2,30], Lavanya Singh[6], Pamela Smith-Lawrence[26], Wendy Stevens[44], Amy Strydom[14], Kathleen Subramoney[32], Naume Tebeila[5], Derek Tshiabuila[6], Joseph Tsui[17], Stephanie van Wyk[39], Steven Weaver[25], Constantinos K. Wibmer[5], Eduan Wilkinson[39], Nicole Wolter[5,45], Alexander E. Zarebski[17], Boitumelo Zuze[2], Dominique Goedhals[10,46], Wolfgang Preiser[19,31], Florette Treurnicht[32], Marietje Venter[14], Carolyn Williamson[16,22,23,47], Oliver G. Pybus[17], Jinal Bhiman[5,7], Allison Glass[1,48], Darren P. Martin[23,47], Andrew Rambaut[13], Simani Gaseitsiwe[2,3,51], Anne von Gottberg[5,45,51] & Tulio de Oliveira[6,39,49,51✉]

The severe acute respiratory syndrome coronavirus 2 (SARS-CoV-2) epidemic in southern Africa has been characterised by three distinct waves. The first was associated with a mix of SARS-CoV-2 lineages, whilst the second and third waves were driven by the Beta and Delta variants, respectively[1–3]. In November 2021, genomic surveillance teams in South Africa and Botswana detected a new SARS-CoV-2 variant associated with a rapid resurgence of infections in Gauteng Province, South Africa. Within three days of the first genome being uploaded, it was designated a variant of concern (Omicron) by the World Health Organization and, within three weeks, had been identified in 87 countries. The Omicron variant is exceptional for carrying over 30 mutations in the spike glycoprotein, predicted to influence antibody neutralization and spike function[4]. Here, we describe the genomic profile and early transmission dynamics of Omicron, highlighting the rapid spread in regions with high levels of population immunity.

Since the onset of the COVID-19 pandemic in December 2019, variants of SARS-CoV-2 have emerged repeatedly. Some variants have spread worldwide and made major contributions to the cyclical infection waves that occur asynchronously in different regions. Between October and December 2020, the world witnessed the emergence of the first variants of concern (VOCs). These variants exhibited increased transmissibility and/or immune evasion properties that threatened global efforts to control the pandemic. Although the Alpha, Beta and Gamma VOCs[2,5] that emerged during this time disseminated globally

and drove epidemic resurgences in many different countries, it was the highly transmissible Delta variant that subsequently displaced all other VOCs in most regions of the world[6]. During its spread, the Delta variant evolved into multiple sub-lineages[7], some of which demonstrated signs of having a growth advantage in certain locations[8], prompting speculation that the next VOC to drive a resurgence of infections would be likely derived from Delta. In October 2021, while Delta was continuing to exhibit high levels of transmission in the Northern hemisphere, a large Delta wave was subsiding in southern Africa. The culmination of

Article

this wave coincided with the emergence of a novel SARS-CoV-2 variant that, within days of its near-simultaneous discovery in four individuals in Botswana, a traveler from South Africa in Hong Kong, and 54 individuals in South Africa, was designated by the World Health Organization as Omicron: the fifth VOC of SARS-CoV-2. Since then and the beginning of 2022, over 100 000 genomes of Omicron have been produced as Omicron has started to dominate SARS-CoV-2 infections in the world.

Epidemic dynamics and detection of Omicron

The three distinct epidemic waves of SARS-CoV-2 experienced by southern African countries were each driven by different variants: the first between June and August 2020 by descendants of the B.1 lineage[1], the second between November 2020 and February 2021 by the Beta VOC[2,9], and the third between May and September 2021 by the Delta VOC[3], with an estimated 2-5% of third wave cases in South Africa attributed to the C.1.2 lineage[10] (Fig. 1A). Serosurveys conducted before the Delta wave suggested high levels of exposure to SARS-CoV-2 (40-60%) in South Africa[11,12], and estimated seroprevalence was >70% in Gauteng in a population-based survey conducted between October and December 2021[13]. The weeks following the third wave in South Africa, between 10 October and 15 November 2021, were marked by lower levels of transmission as indicated by a low incidence of reported COVID-19 cases (100-200 new cases per day) and low (<2%) test positivity rates (Fig. 1A–C).

A rapid increase in COVID-19 cases was observed from mid-November 2021 in Gauteng province, the economic hub of South Africa containing the cities of Tshwane (Pretoria) and Johannesburg. Specifically, rising case numbers and test positivity rates were first noticed in Tshwane, initially associated with outbreaks in higher education settings. This resurgence of cases was accompanied by an increasing frequency of S-gene target failure (SGTF) during TaqPath-based (Thermo Fisher Scientific) diagnostic PCR testing: a phenomenon previously observed with the Alpha variant due to a deletion at amino acid positions 69 and 70 (Δ69-70) in the SARS-CoV-2 spike protein[14]. Given the low prevalence of Alpha in South Africa (Fig. 1A), targeted whole-genome sequencing of these specimens was prioritized.

On 19 November 2021, sequencing results from a batch of 8 SGTF samples collected between 14-16 November 2021 indicated that all were of a new and genetically-distinct lineage of SARS-CoV-2. Further rapid sequencing identified the same variant in 29 of 32 routine diagnostic samples from multiple locations in Gauteng Province, indicating widespread circulation of this new variant by the second week of November. Crucially, this rise immediately preceded a sharp increase in reported case numbers (Fig. 1C, Extended Data Fig. 1). In the following four days, the presence of this lineage was confirmed by sequencing in another two provinces: KwaZulu-Natal (KZN) and the Western Cape (Fig. 1B).

Concurrently in Gaborone, Botswana (<360km from Tshwane), four genomes generated from samples collected on 11 November 2021, and sequenced on 17-18 November 2021 as part of weekly surveillance, displayed an unusual set of mutations. These were reported to the Botswana Ministry of Health and Wellness on 22 November 2021, as "unusual sequences" that were linked to a group of visitors (non-residents) on a diplomatic mission. The sequences were uploaded to GISAID[15,16] on 23 November 2021, and it became apparent that they belonged to a new lineage. A further 15 genomically confirmed cases (not epidemiologically linked to the first four) were identified within the same week from various other locations in Botswana. All of these either had travel links from South Africa, or were contacts of someone with travel links. On 24 November 2021, these SARS-CoV-2 genomes from both South Africa and Botswana were designated as belonging to a new PANGO lineage (B.1.1.529)[17], later divided into sub-lineages aliased BA.1 (the main clade), BA.2 and BA.3. On 26 November 2021, the lineage was designated a VOC and named Omicron by the WHO on the recommendation of the Technical Advisory Group on SARS-CoV-2 Virus Evolution[18]. By the first

week of December 2021, Omicron was causing a rapid and sustained increase in cases in South Africa and Botswana (Fig. 1C, Extended Data Fig. 2 for Botswana). In Gauteng, weekly test positivity rates increased from <1% in the week beginning 31 October, to 16% in the week beginning 21 November 2021, and to 35% in the week beginning 28 November, concurrent with an exponential rise in COVID-19 incidence (Fig. 1C, Extended Data Fig. 1). Nationally, daily case numbers exceeded 22 000 (84% of the peak of the previous wave of infections) by 9 December 2021. At the same time, the proportion of TaqPath PCR tests with SGTF increased rapidly in all provinces of South Africa, reaching ~90% nationally by the week beginning 21 November 2021, strongly indicating that the fourth wave was being driven by Omicron: an indication that has now been confirmed by virus genome sequencing in all provinces (Fig. 1C). Similarly, Botswana experienced a sharp increase in cases, doubling every 2-3 days late November to early December 2021, transitioning from a 7-day moving average of <10 cases/100 000 to above 25 cases/100,000 in less than 10 days (Extended Data Fig. 2).

By 16 December 2021, Omicron had been detected in 87 countries, both in samples from travelers returning from southern Africa, and in samples from routine community testing (Extended Data Fig. 3) and by 1 January 2022, over 100 000 genomes have been produced from over 100 countries and Omicron was becoming the dominant VOC in the world.

Evolutionary origins of Omicron

To determine when and where Omicron likely originated, we analyzed all 686 available Omicron genomes (including 248 from southern Africa and 438 from elsewhere in the world) retrieved from GISAID (date of access 7 December 2021)[15,16], in the context of a global reference set of representative SARS-CoV-2 genomes (n=12,609) collected between December 2019 and November 2021. Preliminary maximum-likelihood phylogenies identified the BA.1/Omicron sequences as a monophyletic clade rooted within the B.1.1 lineage (Nextstrain clade 20B), with no clear basal progenitor (Fig. 2A). Importantly, the BA.1/Omicron cluster is highly phylogenetically distinct from any known VOC or variants of interest (VOI) and from any other lineages known to be circulating in southern Africa (e.g. C.1.2) (Fig. 2A). More recently, two related lineages have emerged (BA.2 and BA.3), both sharing many, but not all of the characteristic mutations of BA.1/Omicron and both having many unique mutations of their own (Extended Data Fig. 4A, B). While BA.2 and BA.3 are evolutionarily linked to BA.1 in that they all branch off of the same B.1.1 node without obvious progenitors, the three sub-lineages evolved independently from one another along separate branches (Extended Data Fig. 4C, D). The earliest specimens of BA.2 and BA.3 were both sampled after the earliest known BA.1 in South Africa (8 November 2021 at the time of writing), on 17 November 2021 in Tshwane (Gauteng) and on 18 November 2021 in a neighbouring province (North West) respectively. We primarily focus here on the BA.1 lineage which is rapidly spreading in multiple countries around the world and is the lineage first officially designated as the Omicron VOC.

Time-calibrated Bayesian phylogenetic analysis of all BA.1 assigned genomes from southern Africa (as of 11 December 2021, n=553) estimated the time when the most recent common ancestor (TMRCA) of the analysed BA.1 lineage sequences existed to be 9 October 2021 (95% highest posterior density [HPD] 30 September - 20 October) with a per-day exponential growth rate of 0.137 (95% HPD 0.099 – 0.175) reflecting a doubling time of 5.1 days (95% HPD 4.0 – 7.0) (Fig. 2B). These estimates are robust to whether the evolutionary rate is estimated from the data or fixed to previously estimated values (Extended Data Table 1). Limiting the analysis to genomes from Gauteng Province only yields a faster growth rate estimate with a doubling time of 2.8 days (95% HPD 2.1 – 4.2) (Extended Data Table 1). Using a phylodynamic model that accounts for variable genome sampling through time (birth-death skyline model, BDSKY[72]) yields a doubling time of BA.1 assigned genomes from South

Africa and Botswana (n=552) of 3.9 (95% HPD 3.5 - 4.3) days with an effective reproduction number (R_e) of 2.79 (95% HPD 2.60 - 2.97) during the period from early November to early December. BDSKY estimated R_e for the Gauteng Province dataset is 3.86 (95% CI 3.43-4.29) and 3.61 (95% CI 3.20-4.02) for the 3-epoch and 4-epoch model respectively (Extended Data Tables 4 & 5). Spatiotemporal phylogeographic analysis indicates that the BA.1/Omicron variant spread from the Gauteng province of South Africa to seven of the eight other provinces and to two regions of Botswana from late October to late November 2021, and shows evidence of more recent transmission within and between other South African provinces (Fig. 2C). However, this does not imply that Omicron originated in Gauteng and these phylogeographic inferences could change as further genomic data accumulates from other locations.

Molecular profile of Omicron

Compared to Wuhan-Hu-1, BA.1/Omicron carries 15 mutations in the spike receptor-binding domain (RBD) (Fig. 3), five of which (G339D, N440K, S477N, T478K, N501Y) have been shown individually to enhance hACE2 binding[19]. Seven of the RBD mutations (K417N, G446S, E484A, Q493R, G496S, Q498R and N501Y) are expected to have moderate to strong impacts on binding of at least three of the four major classes of RBD-targeted neutralizing antibodies (NAbs)[20–22]. These RBD mutations coupled with four amino acid substitutions (A67V, T95I, G142D, and L212I), three deletions (69-70, 143-145 and 211) and an insertion (EPE between 214 and 215) in the N-terminal domain (NTD)[23], are predicted to underlie the substantially reduced sensitivity of Omicron to neutralization by anti-SARS-CoV-2 antibodies induced by either infection or vaccination[24,25]. These mutations also involve key structural epitopes targeted by some of the currently authorized monoclonal antibodies, particularly bamlanivimab + etesevimab and casirivimab + imdevimab[25–28]. Preliminary analysis suggests that although the spike mutations involve a number of T cell and B cell epitopes, the majority of epitopes (>70%) remain unaffected[29].

Omicron also has a cluster of three mutations (H655Y, N679K and P681H) adjacent to the S1/S2 furin cleavage site (FCS) which are likely to enhance spike protein cleavage and fusion with host cells[30,31] and which could also contribute to enhanced transmissibility[32] (Extended Data Fig. 5).

Outside of the spike protein, a deletion in nsp6 (105-107del), in the same region as deletions seen in Alpha, Beta, Gamma and Lambda, may have a role in evasion of innate immunity[33] and the double mutation in nucleocapsid (R203K, G204R), also present in Alpha, Gamma and C.1.2, has been associated with enhanced infectivity in human lung cells[34].

Recombination analysis

Given the large number of mutations differentiating BA.1/Omicron, BA.2 and BA.3 from other known SARS-CoV-2 lineages it was considered plausible that either (i) all of these lineages might have descended from a common recombinant ancestor, (ii) that one or more of the BA lineages might have originated via recombination between a virus in one of the other BA lineages and a virus in a non-BA lineage, or (iii) that one of the BA lineages may have originated through recombination between viruses in the other two BA lineages. We tested these hypotheses using a variety of recombination detection approaches (implemented in the programs GARD[35]; 3SEQ[36]; and RDP5[37]) to identify potential signals of recombination in sequence datasets containing BA.1, BA.2 and BA.3 sequences together with sequences representative of global SARS-CoV-2 genomic diversity.

Potential evidence of a single recombination event involving BA.1, BA.2 and BA3 was identified by 3SEQ (p=0.03), GARD (delta c-AIC = 20) and RDP5 (GENECONV p=0.027; RDP p=0.006). within the NTD encoding region of spike. The most likely breakpoint locations for this recombination event were 21690 for the 5' breakpoint (high likelihood

interval between 15716 and 21761) and 22198 for the 3' breakpoint (high likelihood interval between 22197 and 22774). However, these analyses could not reliably identify which of BA.1, BA.2 or BA.3 was the recombinant. Phylogenetic analysis of the genome regions bounded by these breakpoints (genome coordinates 1-21689, 21690-22198 and 22199-29903) potentially supported: (i) BA.1 having acquired the NTD encoding region of BA.3 through recombination, (ii) BA.3 having acquired the NTD encoding region of BA.1 through recombination or (iii) BA.2 having acquired the NTD encoding region of a non-BA lineage virus through recombination (Extended Data Fig. 6).

Although we found weak statistical and phylogenetic evidence of one of BA.1, BA.2 or BA.3 being recombinant, we found no evidence that the MRCA of the BA.1, BA.2 and BA.3 lineages was recombinant. It should be noted, however, that recombination tests in general will not have sufficient statistical power to reliably identify evidence of individual recombination events that result in transfers of less than ~5 contiguous polymorphic nucleotide sites between genomes[35,38,39]. Further, if BA.1 BA.2 and/or BA.3 are the products of a series of multiple partially overlapping recombination events occurring across multiple temporally clustered replication cycles, the complex patterns of nucleotide variation that might result could be extremely difficult to interpret as recombination using the methods applied here[40].

Selection analysis of Omicron

The large numbers of mutations seen in the BA.1, BA.2 and BA.3 lineage sequences may have accrued at an accelerated pace under the influence of positive selection. To test for evidence of this we applied a selection analysis pipeline to all available sequences designated as BA.1, BA.2, and BA.3 in GISAID as of 20 December 2021. We ran selection screens individually on BA.1, BA.2, and BA.3 sequences, following a previously described procedure[33]. We downsampled alignments of individual protein encoding regions to obtain a median of 110 genetically unique BA.1 sequences, 3 BA.2 sequences, 2.5 BA.3 sequences and ~100 other unique sequences for each gene/ORF from a representative collection of other SARS-CoV-2 lineages (used as background sequences to contextualize evolution within the Omicron sub-clade).

Given that the BA.1 lineage has 1000-fold more sequences than BA.2 and BA.3, we performed the most detailed analysis on it. We detected evidence of gene-wide positive selection (using the BUSTED method[41]) acting on ten genes/ORFs since the ancestral BA.1 lineage split from the B.1.1 lineage: S-gene, exonuclease), M-gene (p = 0.002), N-gene (p = 0.006), RdRp (p=), nsp3 (p = 0.05), methyltransferase, helicase, ORF7a, ORF6, and ORF3a (p<0.0001 for all tests). In all ten genes, this selection was strong (dN/dS > 5), and occurred in bursts (≤ 6% of branch/site combinations selected). The branch separating BA.1 from its most recent B.1.1 ancestor had the most prominent selection signal (which was strongest in the S-gene; with evidence for 9 positively selected sites along this branch[42]), strongly supporting the hypothesis that adaptive evolution played a significant role in the mutational divergence of Omicron from other B.1.1 SARS-CoV-2 lineages. Relative to the intensity of selection evident within the background B.1.1 lineages, selection in three genes was likely significantly intensified in the BA.1 lineage: S-gene (intensification factor K = 2.1; p < 0.0001[43]), exonuclease (K = 3.50; p = 0.0009), nsp6 (K = 2.4; p = 0.03), RdRp (K=1.14, p = 0.02), and M-gene (K=4.6, p < 0.0001)..

Among 1546 codon sites that are polymorphic among the BA.1/Omicron sequences analysed, 45 were found to have experienced episodic positive selection since BA.1 split from the B.1.1 lineage (MEME p ≤ 0.01, Extended Data Table 2[44]). Twenty-three (51%) of these codon sites are in the S-gene, 13 of which contain BA.1 lineage-defining mutations (i.e. these selection signals reflect mutations that occurred within the ancestral Omicron lineage). The three positively selected codon sites that did not correspond to sites of lineage-defining mutations (S/346, S/452, and S/701) are particularly notable as these are attributable to

Article

mutations that have occurred since the MRCA of the analysed BA.1 sequences. The mutations driving the positive selection signals at these three sites in the Omicron S-gene converge on mutations seen in other VOCs or VOIs (R346K in Mu, L452R in Delta, and A701V in Beta and Iota). The A701V mutation, the precise impact of which is currently unknown, is one of 19 in a proposed "501Y lineage Spike meta-signature" comprising the set of mutations that were most adaptive during the evolution of the Alpha, Beta and Gamma VOC lineages[33]. Further, both R346K and L452R are known to impact antibody binding[21] and both of the codon sites where these mutations occur display evidence for directional selection (using the FADE method[45]). These selective patterns suggest that, during its current explosive spread, BA.1/Omicron may be undergoing additional evolution to modify its neutralization profile.

Because the numbers of available BA.2 and BA.3 sequences are much lower than for BA.1, the power to perform selection detection was much reduced and not possible for some genomic regions. Nonetheless, there was a strong signal of selection on the S-gene (p<0.0001 for BA.2 and p = 0.05 for BA.3) and selective pressures on this gene in the BA.2 clade were intensified relative to reference SARS-CoV-2 isolates (K=6.25, p = 0.005). Within BA.2 sequences, positive selection was detectable on five sites in the S-gene (371, 376, 405, 477 and 505 -- all clade defining sites) as well on two sites in the M-gene (19 and 63 -- both clade defining sites). Within BA.3 sequences, positive selection was detectable on four sites in the S-gene (67, 371, 477 and 505 -- all clade defining sites) as well on two sites in the N-gene (13 and 413 -- both clade defining sites).

Transmissibility and immune evasion

We estimated that Omicron had a growth advantage of 0.24 (95% CI: 0.16-0.33) per day over Delta in Gauteng, South Africa (Fig. 4A). This corresponds to a 5.4-fold (95% CI: 3.1-10.1) weekly increase in cases compared to Delta. The growth advantage of Omicron is likely to be mediated by (i) an increase relative to other variants of its intrinsic transmissibility, (ii) an increase relative to other variants in its capacity to infect, and be transmitted from, previously infected and vaccinated individuals; or (iii) both.

The predicted combination of transmissibility and immune evasion for Omicron strongly depends on the assumed level of current population immunity against infection by, and transmission of, the competing variant Delta that is afforded by prior infections with wild-type, Beta, Delta, and other strains during the three previous epidemic waves in South Africa, and/or vaccination (Fig. 4B). For moderate levels of population immunity against Delta ($\Omega = 0.4$), immune evasion alone cannot explain the observed growth advantage of Omicron (Fig. 4C). For medium levels of immunity against Delta ($\Omega = 0.6$), very high levels of immune evasion could explain the observed growth advantage without an additional increase in transmissibility (Fig. 4D). For high levels of population immunity against Delta ($\Omega = 0.8$), even moderate levels of immune evasion (~25-50%) can explain the observed growth advantage without an additional increase in transmissibility (Fig. 4E). The results of seroprevalence studies and vaccination coverage (~40% of the adult population in South Africa suggest that the proportion of the population with potential immunity against Delta and earlier variants is likely to be above 60%[11,12]. We thus argue that the population level of protective immunity against Delta acquired during previous epidemic waves is high, and that partial immune evasion is a major driver for the observed dynamics of Omicron in South Africa. This notion is supported by recent findings that show an increased risk of SARS-CoV-2 reinfection associated with the emergence of Omicron in South Africa[46] and the initial results from neutralization assays[47,48]. In addition to immune evasion, an increase, or decrease, in the transmissibility of Omicron compared to Delta cannot, however, be ruled out.

There are a number of limitations to this analysis. First, we estimated the growth advantage of Omicron based on early sequence data only. These data could be biased due to targeted sequencing of SGTF samples

and stochastic effects (e.g., superspreading) in a low incidence setting, which can lead to overestimates of the growth advantage, and consequently of the increased transmissibility and immune evasion. Second, without reliable estimates of the level of protective immunity against Delta in South Africa, we cannot obtain precise estimates of transmissibility or immune evasion of Omicron.

Conclusion

Strong genomic surveillance systems in South Africa and Botswana enabled the identification of Omicron within a week of observing a resurgence in cases in Gauteng Province. Immediate notification of the WHO and early designation as a VOC has stimulated global scientific efforts and has given other countries time to prepare their response. Omicron is now driving a fourth wave of the SARS-CoV-2 epidemic in southern Africa, and is spreading rapidly in several other countries. Genotypic and phenotypic data suggest that Omicron has the capacity for substantial evasion of neutralizing antibody responses, and modelling suggests that immune evasion could be a major driver of the observed transmission dynamics. Close monitoring of the spread of Omicron in countries outside southern Africa will be necessary to better understand its transmissibility and the capacity of this variant to evade post-infection and vaccine-elicited immunity. Neutralizing antibodies are only one component of the immune protection from vaccines and prior infection, and the cellular immune response is predicted to be less affected by the mutations in Omicron. Vaccination therefore remains critical to protect those at highest risk of severe disease and death. The emergence and rapid spread of Omicron poses a threat to the world and a particular threat in Africa, where fewer than one in ten people are fully vaccinated.

Online content

Any methods, additional references, Nature Research reporting summaries, source data, extended data, supplementary information, acknowledgements, peer review information; details of author contributions and competing interests; and statements of data and code availability are available at https://doi.org/10.1038/s41586-022-04411-y.

1. Tegally, H. et al. Sixteen novel lineages of SARS-CoV-2 in South Africa. *Nat. Med.* **27**, 440–446 (2021).
2. Tegally, H. et al. Detection of a SARS-CoV-2 variant of concern in South Africa. *Nature* **592**, 438–443 (2021).
3. Tegally, H. et al. Rapid replacement of the Beta variant by the Delta variant in South Africa. *medRxiv* (2021) https://doi.org/10.1101/2021.09.23.21264018.
4. Martin, D. P. et al. Selection analysis identifies significant mutational changes in Omicron that are likely to influence both antibody neutralization and Spike function (part 1 of 2). https://virological.org/t/selection-analysis-identifies-significant-mutational-changes-in-omicron-that-are-likely-to-influence-both-antibody-neutralization-and-spike-function-part-1-of-2/771 (2021).
5. Faria, N. R. et al. Genomics and epidemiology of the P.1 SARS-CoV-2 lineage in Manaus, Brazil. *Science* **372**, 815–821 (2021).
6. Dhar, M. S. et al. Genomic characterization and epidemiology of an emerging SARS-CoV-2 variant in Delhi, India. *Science* **374**, 995–999 (2021).
7. New AY lineages – Pango Network. https://www.pango.network/new-ay-lineages/.
8. Eales, O. et al. SARS-CoV-2 lineage dynamics in England from September to November 2021: high diversity of Delta sub-lineages and increased transmissibility of AY.4.2. *medRxiv* (2021).
9. Wilkinson, E. et al. A year of genomic surveillance reveals how the SARS-CoV-2 pandemic unfolded in Africa. *Science* **374**, 423–431 (2021).
10. Scheepers, C. et al. The continuous evolution of SARS-CoV-2 in South Africa: a new lineage with rapid accumulation of mutations of concern and global detection. *medRxiv* (2021) https://doi.org/10.1101/2021.08.20.21262342.
11. Kleynhans, J. et al. SARS-CoV-2 Seroprevalence in a Rural and Urban Household Cohort during First and Second Waves of Infections, South Africa, July 2020-March 2021. *Emerging Infect. Dis.* **27**, 3020–3029 (2021).
12. Vermeulen, M. et al. Prevalence of anti-SARS-CoV-2 antibodies among blood donors in South Africa during the period January-May 2021. *Res. Sq.* (2021) https://doi.org/10.21203/rs.3.rs-690372/v1.
13. Madhi, S. et al. South African Population Immunity and Severe Covid-19 with Omicron Variant. *medRxiv* (2021) https://doi.org/10.1101/2021.12.20.21268096.
14. Volz, E. et al. Assessing transmissibility of SARS-CoV-2 lineage B.1.1.7 in England. *Nature* (2021) https://doi.org/10.1038/s41586-021-03470-x.

15. Shu, Y. & McCauley, J. GISAID: Global initiative on sharing all influenza data - from vision to reality. *Euro Surveill.* **22**, 30494 (2017).

16. Elbe, S. & Buckland-Merrett, G. Data, disease and diplomacy: GISAID's innovative contribution to global health. *Global Challenges* **1**, 33–46 (2017).

17. Rambaut, A. et al. A dynamic nomenclature proposal for SARS-CoV-2 lineages to assist genomic epidemiology. *Nat. Microbiol.* **5**, 1403–1407 (2020).

18. World Health Organization. Classification of Omicron (B.1.1.529): SARS-CoV-2 Variant of Concern. https://www.who.int/news-room/statements/26-11-2021-classification-of-omicron-(b.1.1.529)-sars-cov-2-variant-of-concern (2021).

19. Starr, T. N. et al. Deep Mutational Scanning of SARS-CoV-2 Receptor Binding Domain Reveals Constraints on Folding and ACE2 Binding. *Cell* **182**, 1295-1310.e20 (2020).

20. Greaney, A. J. et al. Mapping mutations to the SARS-CoV-2 RBD that escape binding by different classes of antibodies. *Nat. Commun.* **12**, 4196 (2021).

21. Greaney, A. J. et al. Complete Mapping of Mutations to the SARS-CoV-2 Spike Receptor-Binding Domain that Escape Antibody Recognition. *Cell Host Microbe* **29**, 44-57.e9 (2021).

22. Greaney, A. J. et al. Comprehensive mapping of mutations in the SARS-CoV-2 receptor-binding domain that affect recognition by polyclonal human plasma antibodies. *Cell Host Microbe* **29**, 463-476.e6 (2021).

23. McCallum, M. et al. N-terminal domain antigenic mapping reveals a site of vulnerability for SARS-CoV-2. *Cell* **184**, 2332-2347.e16 (2021).

24. Cele, S. et al. Omicron extensively but incompletely escapes Pfizer BNT162b2 neutralization. *Nature* (2021) https://doi.org/10.1038/d41586-021-03824-5.

25. Planas, D. et al. Considerable escape of SARS-CoV-2 Omicron to antibody neutralization. *Nature* (2021) https://doi.org/10.1038/d41586-021-03827-2.

26. Starr, T. N., Greaney, A. J., Dingens, A. S. & Bloom, J. D. Complete map of SARS-CoV-2 RBD mutations that escape the monoclonal antibody LY-CoV555 and its cocktail with LY-CoV016. *Cell Rep. Med.* **2**, 100255 (2021).

27. Starr, T. N. et al. Prospective mapping of viral mutations that escape antibodies used to treat COVID-19. *Science* **371**, 850–854 (2021).

28. Cao, Y. et al. Omicron escapes the majority of existing SARS-CoV-2 neutralizing antibodies. *Nature* (2021) https://doi.org/10.1038/d41586-021-03796-6.

29. Keeton, R. et al. SARS-CoV-2 spike T cell responses induced upon vaccination or infection remain robust against Omicron. *medRxiv* 2021.12.26.21268380 (2021).

30. Brown, J. C. et al. Increased transmission of SARS-CoV-2 lineage B.1.1.7 (VOC 2020212/01) is not accounted for by a replicative advantage in primary airway cells or antibody escape. *BioRxiv* (2021) https://doi.org/10.1101/2021.02.24.432576.

31. Saito, A. et al. SARS-CoV-2 spike P681R mutation enhances and accelerates viral fusion. *BioRxiv* (2021) https://doi.org/10.1101/2021.06.17.448820.

32. Mlcochova, P. et al. SARS-CoV-2 B.1.617.2 Delta variant replication and immune evasion. *Nature* **599**, 114–119 (2021).

33. Martin, D. P. et al. The emergence and ongoing convergent evolution of the SARS-CoV-2 N501Y lineages. *Cell* **184**, 5189-5200.e7 (2021).

34. Wu, H. et al. Nucleocapsid mutations R203K/G204R increase the infectivity, fitness, and virulence of SARS-CoV-2. *Cell Host Microbe* (2021) https://doi.org/10.1016/j.chom.2021.11.005.

35. Kosakovsky Pond, S. L., Posada, D., Gravenor, M. B., Woelk, C. H. & Frost, S. D. W. GARD: a genetic algorithm for recombination detection. *Bioinformatics* **22**, 3096–3098 (2006).

36. Lam, H. M., Ratmann, O. & Boni, M. F. Improved algorithmic complexity for the 3SEQ recombination detection algorithm. *Mol. Biol. Evol.* **35**, 247–251 (2018).

37. Martin, D. P. et al. RDP5: a computer program for analyzing recombination in, and removing signals of recombination from, nucleotide sequence datasets. *Virus Evol.* **7**, veaa087 (2021).

38. Boni, M. F., Posada, D. & Feldman, M. W. An exact nonparametric method for inferring mosaic structure in sequence triplets. *Genetics* **176**, 1035–1047 (2007).

39. Posada, D. & Crandall, K. A. Evaluation of methods for detecting recombination from DNA sequences: computer simulations. *Proc Natl Acad Sci USA* **98**, 13757–13762 (2001).

40. van der Walt, E. et al. Rapid host adaptation by extensive recombination. *J. Gen. Virol.* **90**, 734–746 (2009).

41. Wisotsky, S. R., Kosakovsky Pond, S. L., Shank, S. D. & Muse, S. V. Synonymous Site-to-Site Substitution Rate Variation Dramatically Inflates False Positive Rates of Selection Analyses: Ignore at Your Own Peril. *Mol. Biol. Evol.* **37**, 2430–2439 (2020).

42. Smith, M. D. et al. Less is more: an adaptive branch-site random effects model for efficient detection of episodic diversifying selection. *Mol. Biol. Evol.* **32**, 1342–1353 (2015).

43. Wertheim, J. O., Murrell, B., Smith, M. D., Kosakovsky Pond, S. L. & Scheffler, K. RELAX: detecting relaxed selection in a phylogenetic framework. *Mol. Biol. Evol.* **32**, 820–832 (2015).

44. Murrell, B. et al. Detecting individual sites subject to episodic diversifying selection. *PLoS Genet.* **8**, e1002764 (2012).

45. Kosakovsky Pond, S. L., Poon, A. F. Y., Leigh Brown, A. J. & Frost, S. D. W. A maximum likelihood method for detecting directional evolution in protein sequences and its application to influenza A virus. *Mol. Biol. Evol.* **25**, 1809–1824 (2008).

46. Pulliam, J. R. C. et al. SARS-CoV-2 reinfection trends in South Africa: analysis of routine surveillance data. *medRxiv* (2021) https://doi.org/10.1101/2021.11.11.21266068.

47. Rössler, A., Riepler, L., Bante, D., Laer, D. von & Kimpel, J. SARS-CoV-2 B.1.1.529 variant (Omicron) evades neutralization by sera from vaccinated and convalescent individuals. *medRxiv* (2021) https://doi.org/10.1101/2021.12.08.21267491.

48. Cele, S. et al. SARS-CoV-2 Omicron has extensive but incomplete escape of Pfizer BNT162b2 elicited neutralization and requires ACE2 for infection. *medRxiv* (2021) https://doi.org/10.1101/2021.12.08.21267417.

72. Stadler, T., Kühnert, D., Bonhoeffer, S. & Drummond, A. J. Birth-death skyline plot reveals temporal changes of epidemic spread in HIV and hepatitis C virus (HCV). *Proc Natl Acad Sci USA* **110**, 228–233 (2013).

[1]Lancet Laboratories, Johannesburg, South Africa. [2]Botswana Harvard AIDS Institute Partnership, Botswana Harvard HIV Reference Laboratory, Gaborone, Botswana. [3]Harvard T.H. Chan School of Public Health, Boston, MA, USA. [4]Botswana Presidential COVID-19 Taskforce, Gaborone, Botswana. [5]National Institute for Communicable Diseases (NICD) of the National Health Laboratory Service (NHLS), Johannesburg, South Africa. [6]KwaZulu-Natal Research Innovation and Sequencing Platform (KRISP), Nelson R Mandela School of Medicine, University of KwaZulu-Natal, Durban, South Africa. [7]South African Medical Research Council Antibody Immunity Research Unit, School of Pathology, Faculty of Health Sciences, University of the Witwatersrand, Johannesburg, South Africa. [8]Institute of Social and Preventive Medicine, University of Bern, Bern, Switzerland. [9]Division of Virology, National Health Laboratory Service, Bloemfontein, South Africa. [10]Division of Virology, University of the Free State, Bloemfontein, South Africa. [11]Center for Infectious Disease Dynamics, Department of Biology, Pennsylvania State University, University Park, PA, USA. [12]Diagnofirm Medical Laboratories, Gaborone, Botswana. [13]Institute of Evolutionary Biology, University of Edinburgh, Edinburgh, UK. [14]Zoonotic Arbo and Respiratory Virus Program, Centre for Viral Zoonoses, Department of Medical Virology, University of Pretoria, Pretoria, South Africa. [15]Emweb bv, Herent, Belgium. [16]Division of Medical Virology, Faculty of Health Sciences, University of Cape Town, Cape Town, South Africa. [17]Department of Zoology, University of Oxford, Oxford, UK. [18]Department of Biosystems Science and Engineering, ETH Zurich, Zurich, Switzerland. [19]Division of Medical Virology, Faculty of Medicine and Health Sciences, Stellenbosch University, Tygerberg, Cape Town, South Africa. [20]Laboratorio de Flavivirus, Fundacao Oswaldo Cruz, Rio de Janeiro, Brazil. [21]Laboratório de Genética Celular e Molecular, Universidade Federal de Minas Gerais, Belo Horizonte, Brazil. [22]Division of Virology, NHLS Groote Schuur Laboratory, Cape Town, South Africa. [23]Wellcome Centre for Infectious Diseases Research in Africa (CIDRI-Africa), Cape Town, South Africa. [24]Division of Computational Biology, Faculty of Health Sciences, University of Cape Town, Cape Town, South Africa. [25]Institute for Genomics and Evolutionary Medicine, Department of Biology, Temple University, Philadelphia, Pennsylvania, USA. [26]Health Services Management, Ministry of Health and Wellness, Gaborone, Botswana. [27]NHLS Port Elizabeth Laboratory, Port Elizabeth, South Africa. [28]Faculty of Health Sciences, Walter Sisulu University, Eastern Cape, South Africa. [29]Public Health Department, Integrated Disease Surveillance and Response, Ministry of Health and Wellness, Gaborone, Botswana. [30]Department of Immunology and Infectious Diseases, Harvard T.H. Chan School of Public Health, Boston, Massachusetts, USA. [31]NHLS Tygerberg Laboratory, Tygerberg, Cape Town, South Africa. [32]Department of Virology, Charlotte Maxeke Johannesburg Academic Hospital, Johannesburg, South Africa. [33]Botswana-Baylor Children's Clinical Centre of Excellence, Gaborone, Botswana. [34]Baylor College of Medicine, Houston, Texas, USA. [35]Department of Medical Virology, University of Pretoria, Pretoria, South Africa. [36]National Health Laboratory, Health Services Management, Ministry of Health and Wellness, Gaborone, Botswana. [37]National Health Laboratory Service (NHLS), Johannesburg, South Africa. [38]Centre for the AIDS Programme of Research in South Africa (CAPRISA), Durban, South Africa. [39]Centre for Epidemic Response and Innovation (CERI), School of Data Science and Computational Thinking, Stellenbosch University, Stellenbosch, South Africa. [40]Department of Medicine, Faculty of Medicine, University of Botswana, Gaborone, Botswana. [41]Department of Medical Laboratory Sciences, School of Allied Health Professions, Faculty of Health Sciences, University of Botswana, Gaborone, Botswana. [42]Discipline of Virology, School of Laboratory Medicine and Medical Sciences and National Health Laboratory Service (NHLS), University of KwaZulu–Natal, Durban, South Africa. [43]Next Generation Sequencing Unit, Division of Virology, Faculty of Health Sciences, University of the Free State, Bloemfontein, South Africa. [44]Department of Molecular Medicine and Haematology, University of the Witwatersrand, Johannesburg, South Africa. [45]School of Pathology, Faculty of Health Sciences, University of the Witwatersrand, Johannesburg, South Africa. [46]PathCare Vermaak, Pretoria, South Africa. [47]Institute of Infectious Disease and Molecular Medicine, University of Cape Town, Cape Town, South Africa. [48]Department of Molecular Pathology, School of Pathology, Faculty of Health Sciences, University of the Witwatersrand, Johannesburg, South Africa. [49]Department of Global Health, University of Washington, Seattle, WA, USA. [50]These authors contributed equally: Raquel Viana, Sikhulile Moyo, Daniel G Amoako, Houriiyah Tegally, Cathrine Scheepers. [51]These authors jointly supervised the work: Simani Gaseitsiwe, Anne von Gottberg, Tulio de Oliveira. ✉e-mail: tulio@sun.ac.za
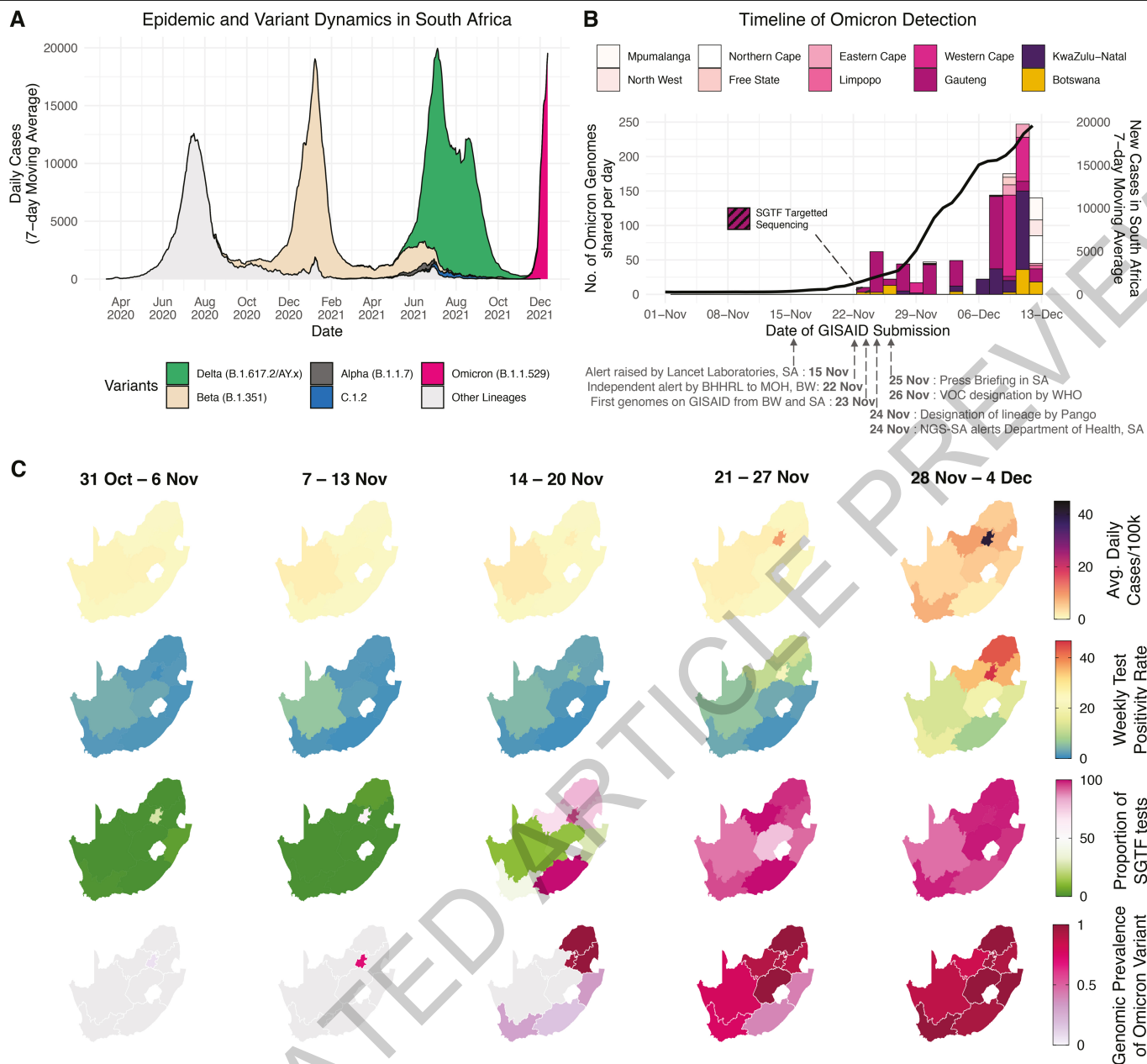
Fig. 1 | Detection of Omicron variant. A) The progression of daily reported cases in South Africa from March 2020 to December 2021. The 7-day rolling average of daily case numbers is coloured by the inferred proportion of variants responsible for the infections, as calculated by genomic surveillance data on GISAID. B) Timeline of Omicron detection in Botswana and South Africa. Bars represent the number of Omicron genomes shared per day, according to the date they were uploaded to GISAID, while the line represents the 7-day moving average of daily new cases in South Africa. C) Weekly progression of average daily cases per 100,000, test positivity rates, proportion of SGTF tests (on the TaqPath COVID-19 PCR assay) and genomic prevalence of Omicron in nine provinces of South Africa for five weeks from 31 October to 4 December 2021. Note that because of heterogeneous use of the TaqPath PCR assay across provinces, the proportion of SGTF tests illustrated for the Eastern Cape Province in weeks of 14 - 20 Nov and 21 - 27 Nov are based on only 2 and 4 data points respectively. Genomic prevalence here is equivalent to the proportion of weekly surveillance sequences genotyped as being Omicron.
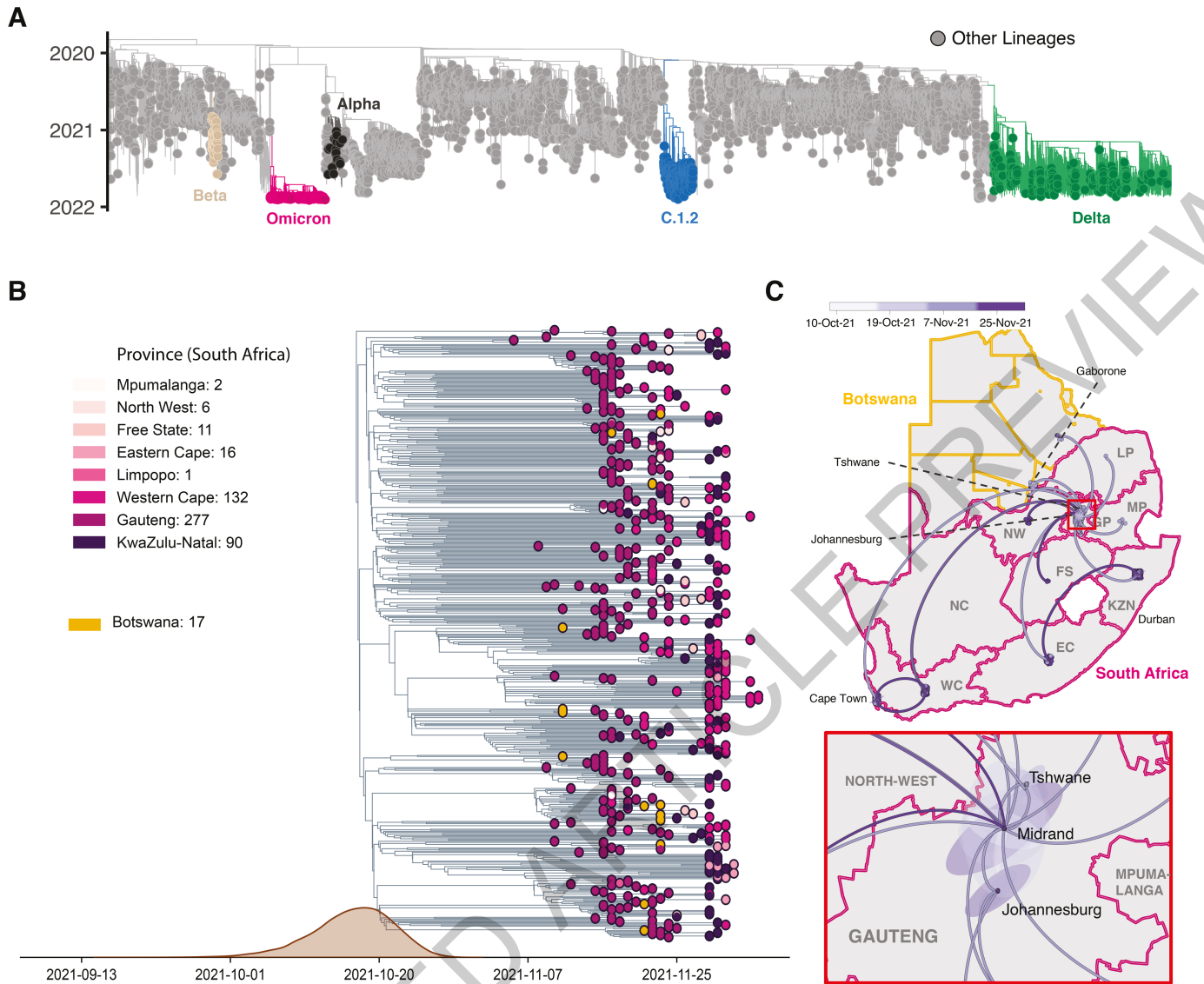
Fig. 2 | Evolution of Omicron. A) Time-resolved maximum likelihood phylogeny of 13,295 SARS-CoV-2 genomes; 9,944 of these are from Africa (denoted with tip point circle shapes). Alpha, Beta and Delta VOCs and the C.1.2 lineage, recently circulating in South Africa, are denoted in black, brown, green and blue respectively. The newly identified SARS-CoV-2 Omicron variant is shown in pink. Genomes of other lineages are shown in grey. B) Time-resolved maximum clade credibility phylogeny of the Omicron cluster of southern African genomes (n = 553), with locations indicated. The posterior distribution of the TMRCA is also shown. C) Spatiotemporal reconstruction of the spread of the Omicron variant in Southern Africa with an inset of Gauteng province. Circles represent nodes of the maximum clade credibility phylogeny, coloured according to their inferred time of occurrence (scale in top panel). Shaded areas represent the 80% highest posterior density interval and depict the uncertainty of the phylogeographic estimates for each node. Solid curved lines denote the links between nodes and the directionality of movement is anticlockwise along the curve.

A
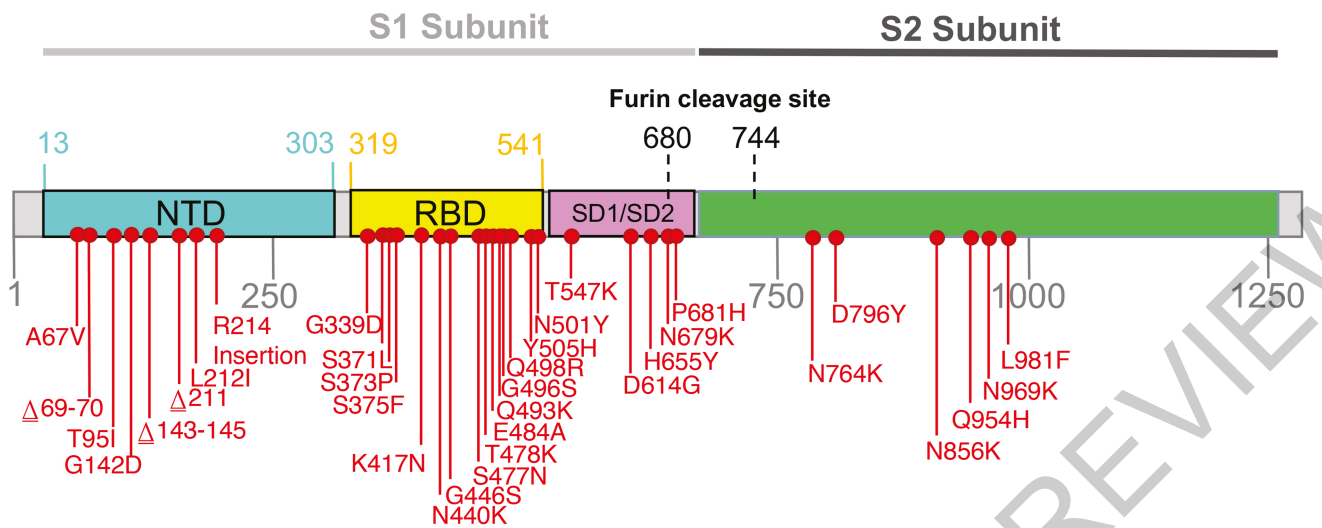
B
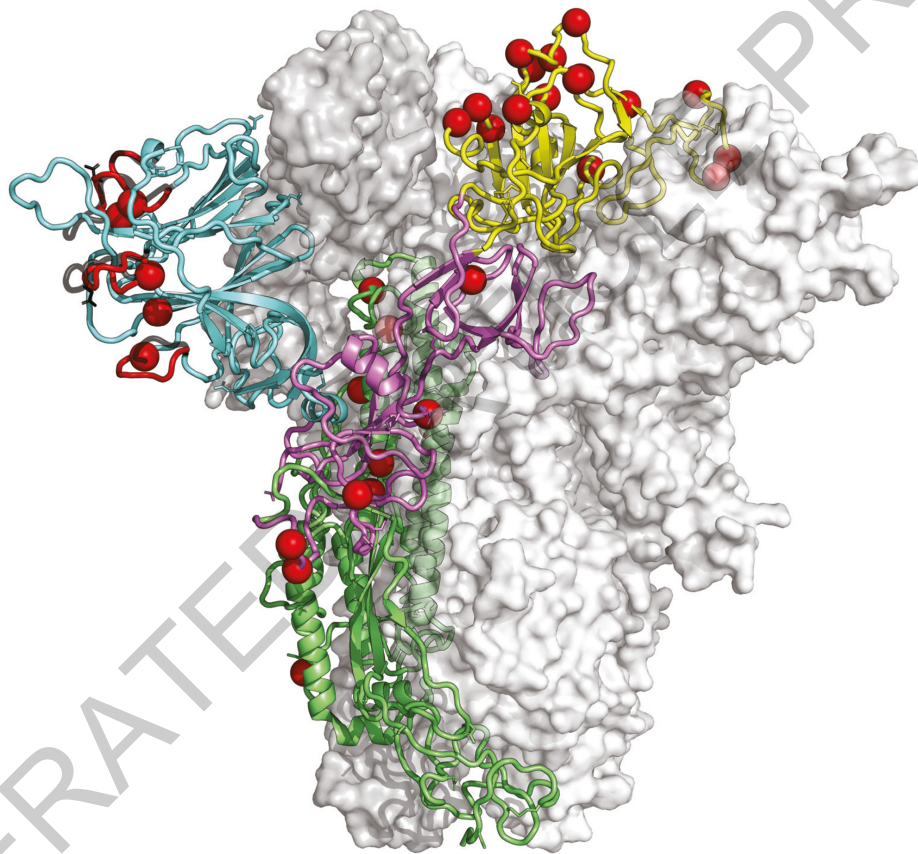
Fig. 3 | Molecular profile of BA.1/Omicron. A) Amino-acid mutations on the spike gene of the BA.1/Omicron variant. B) Structure of the SARS-CoV-2 Spike trimer, showing a single spike protomer in cartoon view. The N terminal domain, receptor binding domain, subdomains 1 and 2, and the S2 protein are shown in cyan, yellow, pink, and green respectively. Red spheres indicate the alpha carbon positions for each omicron variant residue. NTD-specific loop insertions/deletions are shown in red, with the original loop shown in transparent black.
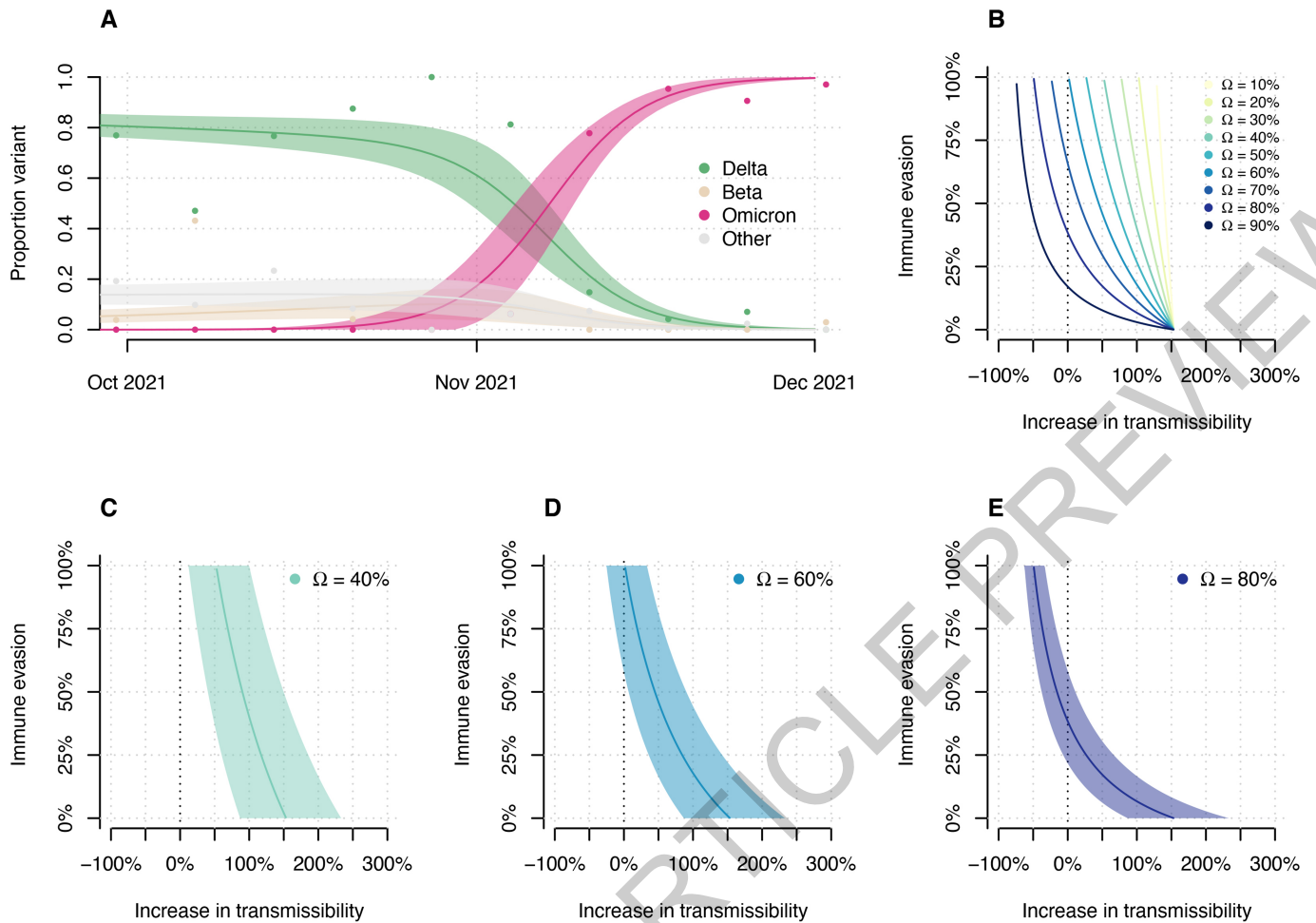
Fig. 4 | Growth of Omicron in Gauteng, South Africa, and relationship between potential increase in transmissibility and immune evasion. (A) Omicron rapidly outcompeted Delta in November 2021. Model fits are based on a multinomial logistic regression. Dots represent the weekly proportions of variants. (B) The relationship between the potential increase in transmissibility and immune evasion strongly depends on the assumed level of current population immunity against Delta that is afforded by prior-infections during earlier epidemic waves and/or vaccination (Ω). (C–E) Relationship for a population immunity of 40%, 60%, and 80% against infection and transmission with Delta. The dark vertical dashed line indicates equal transmissibility of Omicron compared to Delta. Shaded areas correspond to the 95% CIs of the model estimates.

Article

Methods

Epidemiological dynamics

We analyzed daily cases of SARS-CoV-2 in South Africa up to 14 December 2021 from publicly released data provided by the National Department of Health and the National Institute for Communicable Diseases. This was accessible through the repository of the Data Science for Social Impact Research Group at the University of Pretoria (https://github.com/dsfsi/covid19za)[49,50]. The National Department of Health releases daily updates on the number of confirmed new cases, deaths and recoveries, with a breakdown by province. Daily case numbers for Botswana were obtained via Our World in Data (OWID) COVID-19 data repository (https://github.com/owid/covid-19-data). We obtained test positivity data from weekly reports from the National Institute for Communicable Diseases (NICD)[51]. Data to calculate the proportion of positive Thermo Fisher TaqPath COVID-19 PCR tests with SGTF in South Africa was obtained from the National Health Laboratory Service and Lancet Laboratories. Test positivity data for Botswana was obtained from the National Health Laboratory through 6 December 2021. All data visualization was generated through the ggplot package in R[52].

SARS-CoV-2 sampling

As part of the NGS-SA, seven sequencing hubs in South Africa receive randomly selected samples for sequencing every week according to approved protocols at each site[53]. These samples include remnant nucleic acid extracts or remnant nasopharyngeal and oropharyngeal swab samples from routine diagnostic SARS-CoV-2 PCR testing from public and private laboratories in South Africa. In response to a focal resurgence of COVID-19 in the City of Tshwane Metropolitan Municipality in Gauteng Province in November, we enriched our routine sampling with additional samples from the affected area, including initial targeted sequencing of SGTF samples. In Botswana, all public and private laboratories submit randomly selected residual nasopharyngeal and oropharyngeal PCR positive samples weekly to the National Health Laboratory (NHL) and the Botswana Harvard HIV Reference Laboratory (BHHRL) for sequencing.

Ethical statement

The genomic surveillance in South Africa was approved by the University of KwaZulu–Natal Biomedical Research Ethics Committee (BREC/00001510/2020), the University of the Witwatersrand Human Research Ethics Committee (HREC) (M180832), Stellenbosch University HREC (N20/04/008_COVID-19), University of Cape Town HREC (383/2020), University of Pretoria HREC (H101/17) and the University of the Free State Health Sciences Research Ethics Committee (UFS-HSD2020/1860/2710). The genomic sequencing in Botswana was conducted as part of the national vaccine roll-out plan and was approved by the Health Research and Development Committee (Health Research Ethics body, HRDC#00948 and HRDC#00904). Individual participant consent was not required for the genomic surveillance. This requirement was waived by the Research Ethics Committees.

Ion Torrent Genexus Integrated Sequencer methodology for rapid whole genome sequencing of SARS-CoV-2

Viral RNA was extracted using the MagNA Pure 96 DNA and Viral Nucleic Acid kit on the automated MagNA Pure 96 system (Roche Diagnostics, USA) as per the manufacturer's instructions. Extracts were then screened by qPCR to acquire the mean cycle threshold (Ct) values for the SARS-CoV-2 N-gene and ORF1ab-gene using the TaqMan 2019-nCoV assay kit v1 (ThermoFisher Scientific, USA) on the ViiA7 Real-time PCR system (ThermoFisher Scientific, USA) as per the manufacturer's instructions. Extracts were sorted into batches of N=8 within a Ct range difference of 5 for a maximum of two batches per run. Extracts with <200 copies were sequenced using the low viral titer protocol. Next-generation sequencing was performed using the Ion AmpliSeq SARS-CoV-2 Research Panel on the Ion Torrent Genexus Integrated Sequencer (ThermoFisher Scientific, USA) which combines automated cDNA synthesis, library preparation, templating preparation and sequencing within 24 hours. The Ion Ampliseq SARS-CoV-2 Research Panel consists of 2 primer pools targeting 237 amplicons tiled across the SARS-CoV-2 genome providing >99% coverage of the SARS-CoV-2 genome (~30 kb) and an additional 5 primer pairs targeting human expression controls. The SARS-CoV-2 amplicons range from 125 to 275 bp in length. TRINITY was utilised for de novo assembly and the Iterative Refinement Meta-Assembler (IRMA) for genome assisted assembly as well as FastQC for quality checks.

Whole-genome sequencing and genome assembly

RNA was extracted on an automated Chemagic 360 instrument, using the CMG-1049 kit (Perkin Elmer, Hamburg, Germany). The RNA was stored at −80 ∘C prior to use. Libraries for whole genome sequencing were prepared using either the Oxford Nanopore Midnight protocol with Rapid Barcoding or the Illumina COVIDseq Assay.

Illumina Miseq/NextSeq. For the Illumina COVIDseq assay, the libraries were prepared according to the manufacturer's protocol. Briefly, amplicons were tagmented, followed by indexing using the Nextera UD Indexes Set A. Sequencing libraries were pooled, normalized to 4 nM and denatured with 0.2 N sodium acetate. A 8 pM sample library was spiked with 1% PhiX (PhiX Control v3 adaptor-ligated library used as a control). We sequenced libraries on a 500-cycle v2 MiSeq Reagent Kit on the Illumina MiSeq instrument (Illumina). On the Illumina NextSeq 550 instrument, sequencing was performed using the Illumina COVID-Seq protocol (Illumina Inc, USA), an amplicon-based next-generation sequencing approach. The first strand synthesis was carried using random hexamers primers from Illumina and the synthesized cDNA underwent two separate multiplex PCR reactions. The pooled PCR amplified products were processed for tagmentation and adapter ligation using IDT for Illumina Nextera UD Indexes. Further enrichment and cleanup was performed as per protocols provided by the manufacturer (Illumina Inc). Pooled samples were quantified using Qubit 3.0 or 4.0 fluorometer (Invitrogen Inc.) using the Qubit dsDNA High Sensitivity assay according to manufacturer's instructions. The fragment sizes were analyzed using TapeStation 4200 (Invitrogen). The pooled libraries were further normalized to 4nM concentration and 25 μl of each normalized pool containing unique index adapter sets were combined in a new tube. The final library pool was denatured and neutralized with 0.2N sodium hydroxide and 200 mM Tris-HCL (pH7), respectively. 1.5 pM sample library was spiked with 2% PhiX. Libraries were loaded onto a 300-cycle NextSeq 500/550 HighOutput Kit v2 and run on the Illumina NextSeq 550 instrument (Illumina, San Diego, CA, USA).

Midnight Protocol. For Oxford Nanopore sequencing, the Midnight primer kit was used as described by Freed and Silander[54]. cDNA synthesis was performed on the extracted RNA using LunaScript RT mastermix (New England BioLabs) followed by gene-specific multiplex PCR using the Midnight Primer pools which produce 1200bp amplicons which overlap to cover the 30-kb SARS-CoV-2 genome. Amplicons from each pool were pooled and used neat for barcoding with the Oxford Nanopore Rapid Barcoding kit as per the manufacturer's protocol. Barcoded samples were pooled and bead-purified. After the bead clean-up, the library was loaded on a prepared R9.4.1 flow-cell. A GridION X5 or MinION sequencing run was initiated using MinKNOW software with the base-call setting switched off.

Genome assembly. We assembled paired-end and nanopore .fastq reads using Genome Detective 1.132 (https://www.genomedetective.com) which was updated for the accurate assembly and variant calling of tiled primer amplicon Illumina or Oxford Nanopore reads, and the Coronavirus Typing Tool[55]. For Illumina assembly, GATK

HaploTypeCaller --min-pruning 0 argument was added to increase mutation calling sensitivity near sequencing gaps. For Nanopore, low coverage regions with poor alignment quality (<85% variant homogeneity) near sequencing/amplicon ends were masked to be robust against primer drop-out experienced in the Spike gene, and the sensitivity for detecting short inserts using a region-local global alignment of reads, was increased. In addition, we also used the wf_artic (ARTIC SARS-CoV-2) pipeline as built using the nextflow workflow framework[56]. In some instances, mutations were confirmed visually with .bam files using Geneious software V2020.1.2 (Biomatters). The reference genome used throughout the assembly process was NC_045512.2 (numbering equivalent to MN908947.3).

Raw reads from the Illumina COVIDSeq protocol were assembled using the Exatype NGS SARS-CoV-2 pipeline v1.6.1, (https://sars-cov-2.exatype.com/). This pipeline performs quality control on reads and then maps the reads to a reference using Examap. The reference genome used throughout the assembly process was NC_045512.2 (Accession number: MN908947.3).

Several of the initial Ion Torrent genomes contained a number of frameshifts, which caused unknown variant calls. Manual inspection revealed that these were likely to be sequencing errors resulting in mis-assembled regions (likely due to the known error profile of Ion Torrent sequencers)[57]. To resolve this, the raw reads from the IonTorrent platform were assembled using the SARSCoV2 RECoVERY (REconstruction of COronaVirus gEnomes & Rapid analYsis) pipeline implemented in the Galaxy instance ARIES (https://aries.iss.it). This pipeline fixed the observed frameshifts, confirming that they were artefacts of mis-assembly; this subsequently resolved the variant calls. The Exatype and RECoVERY pipelines each produce a consensus sequence for each sample. These consensus sequences were manually inspected and polished using Aliview v1.27 (http://ormbunkar.se/aliview/).

All of the sequences were deposited in GISAID (https://www.gisaid.org/)[15,16], and the GISAID accession identifiers are included in Supplementary Table 1. Raw reads for our sequences have also been deposited at the NCBI Sequence Read Archive (BioProject accession PRJNA784038).

The number and position of the Omicron mutations has affected a number of primers and caused primer drop-outs across a range of sequencing protocols, especially within the RBD (https://primer-monitor.neb.com/lineages). These primer drop-outs have resulted in a number of genomes missing stretches of the RBD, and can affect estimates of mutation prevalence and the determination of the true set of lineage-defining mutations. Given this, .bam files of all initial genomes were inspected with IG Viewer to confirm mutation calls where reference calls were suspected to be from low coverage at primer dropout sites[58].

Lineage classification. We used the widespread dynamic lineage classification method from the 'Phylogenetic Assignment of Named Global Outbreak Lineages' (PANGOLIN) software suite (https://github.com/hCoV-2019/pangolin)[17]. This is aimed at identifying the most epidemiologically important lineages of SARS-CoV-2 at the time of analysis, enabling researchers to monitor the epidemic in a particular geographic region. For the Omicron variant described in this study, the corresponding PANGO lineage designation is BA.1 (lineages v1.2.106). When first characterized the lineage was designated as B.1.1.529 but the emergence of of three sibling lineages to Omicron resulted in the split into sub-lineages (B.1.1.529.1, B.1.1.529.2 and B.1.1.529.3, aliased as BA.1, BA.2 and BA.3). BA.1 contains all the genomes with the original mutational constellation that was designated as Omicron and, at time of writing, is the dominant sub-lineage.

Recombination testing. To test for the possibility that the Omicron lineage (including BA.1, BA.2 and BA.3) is a recombinant of other SARS-CoV-2 lineages, we used a global subsample of sequences spanning January 2021 to August 2021. Using the NCBI SARS-CoV-2 Data hub[59,60], we constructed a dataset containing 221 sequences by randomly sampling five sequences from each month for each continent. No Oceania samples were available from July or August, and no South American sequences were available from July 2021[61]. These sequences were aligned together with a set of five high quality BA.1, six BA.2 and one BA.3 sequences (representing the known diversity of these clades on 5 December 2021) using MAFFT[62] with default settings. Whereas 3SEQ[36], and RDP5[37] were used to analyse this dataset, a subsample of the 39 most divergent sequences from the dataset was analysed using the GARD recombination detection method[35]. SInce none of these recombination detection methods normally utilize potentially informative deletion patterns, deletions in these alignments were recoded as nucleotide substitutions (one substitution per contiguous run of deleted nucleotides). Further, to minimize multiple testing issues, BA.1, BA.2 or BA.3 were tested for evidence of recombination among one another using individual sequences from each of these lineages (CERI-KRISP-K032254, EPI_ISL_7190366 and EPI_ISL_7526186 respectively) together with the Wuhan-Hu-1 sequence (which served as a reference point for rooting the four taxon phylogeny). Default program settings were used throughout for recombination analyses, with the exception of RDP5 analysis, in which sequences were treated as linear and the window sizes for the SiScan and BootScan methods (two of the seven recombination detection methods applied in RDP5) were changed to 2000 nucleotides.

Selection analyses. We investigated the nature and extent of selective forces acting on BA.1, BA.2 and BA.3 genes encoding individual protein products (respectively, a median of 110, 3 and 2.5 unique BA.1, BA.2 and BA.3 sequences per protein product encoding genome region). A subset of publicly available sequences (from the Virus Pathogen Database and Analysis Resource (ViPR) (https://www.viprbrc.org/) were included as background sequences to contextualize selection signals detectable within the BA.1, BA.2 and BA.3 lineages at the levels of complete protein product encoding regions, and individual codons (a median of ~100 sequences per protein coding region). Sequences were selected, quality checked, aligned and subjected to BUSTED, RELAX, MEME, FADE, FEL, and BGM selection analyses (all implemented in HyPhy v2.5.33[63]) using the automated RASCL pipeline as outlined previously[2,9,33].

Structure modeling. We modelled the spike protein on the basis of the Protein Data Bank coordinate set 7A94, showing the first step of the spike protein trimer activation with one RBD domain in the up position, bound to the human ACE2 receptor[64]. We used the Pymol program (The PyMOL Molecular Graphics System, version 2.2.0) for visualization.

Phylogenetic analysis. All sequences on GISAID[15,16] designated Omicron (n=686; date of access: 7 December 2021) were analyzed against a globally representative reference set of SARS-CoV-2 genotypes (n=12 609) spanning the entire genetic diversity observed since the start of the pandemic. In short, the reference set included: 1. All genomes from Africa assigned to PANGO lineage B.1.1 or any of its descendents, excluding those belonging to a VOC clade; 2. A representative subsampling of global data from the publicly maintained global build of Nextstrain (https://nextstrain.org/ncov/gisaid/global); 3. The top thirty BLAST hits when querying GISAID BLAST for BA.1 and BA.2 sequences. This sampling scheme ensures that we analyze Omicron against the closest variants of the virus. Omicron and reference sequences were aligned with Nextalign[65]. A maximum-likelihood (ML) tree topology was inferred in FastTree[66] under the following parameters: a General Time Reversible (GTR) model of nucleotide substitution and a total of 100 bootstrap replicates[67]. The resulting ML-tree topology was transformed into a time-calibrated phylogeny where branches along the tree are scaled in calendar time using TreeTime[68]. The resulting tree was then visualized and annotated in ggtree in R[69]. Additional BA.2 (n=148) and

BA.3 (n=19) sequences were added to the above phylogeny after review to clarify the evolutionary relationship between BA.1, BA.2 and BA.3 (Extended Data Fig. XC, XD).

Time-calibrated BEAST analysis. To estimate a time-scale and growth rate from the genome sequence data, BEAST v1.10.4[70,71] was used to sample phylogenetic trees under an exponential growth coalescent model using a strict molecular clock. All BA.1 assigned genomes from South Africa and Botswana (as of 11 December 2021) were included, with some lower coverage genomes removed, leaving a total of 553 genomes. The single South African BA.2 genome (CERI-KRISP-K032307, EPI_ISL_6795834) was included to help stabilize the root of the BA.1 clade but the exponential growth coalescent model was only applied to BA.1 (a constant population size coalescent was used for the rest of the tree). The rate of molecular evolution was estimated from the data. Two runs of 100 million iterations were compared to assess convergence and then post-burnin samples pooled to summarize parameter estimates.

Birth-death phylogenetic analysis. We analysed the full South Africa and Botswana dataset (n = 552, all BA.1 assigned), and the reduced dataset containing only Gauteng Province genomes (n = 277) using the serially sampled birth-death skyline (BDSKY) model[72], implemented in BEAST2 v2.5.2[73]. To allow for changes in genomic sampling intensity shortly after the discovery of the new lineage, we allowed the sampling proportion to vary with time while keeping all other models parameters constant over the study period. The choice of prior distributions for the model parameters is summarised in Extended Data Table 3.

For each analysis, we used an HKY substitution model and a strict clock model with a fixed clock rate of 0.75x10^{-3} and 1.1x10^{-3} substitutions/site/year (s/s/y) for the full South Africa and Botswana dataset, and Gauteng Province only dataset, respectively. To allow for comparisons with the exponential growth coalescent model, we additionally repeated the analyses with clock rates fixed at those estimated from the coalescent analyses (1.2x10^{-3} and 0.3x10^{-3} s/s/y). The mean duration of infectiousness was fixed at 10 days[74,75]. The effective reproduction number, R_e, was assumed to be constant through time. The sampling proportion was assumed to be 0 before the collection time of the oldest sample and allowed to change at fixed times that were approximately equidistantly spaced between the oldest sample and the most recent sample. For MCMC analyses of the full South Africa and Botswana dataset, the maximum clade credibility (MCC) tree from the exponential growth coalescent model was used as the starting tree. We kept the tree topology fixed, only estimating internal node heights.

To assess the robustness of our estimates of R_e under different assumptions of temporal variations in the sampling proportion, we repeated the analyses with 3 instead of 4 equidistant change-time points. All other model parameters and priors were kept the same.

For each analysis, we ran two independent chains of 100 million MCMC steps and sampled parameters every 10,000 steps. We used Tracer v1.7[76] to evaluate MCMC convergence for each of the individual chains (ESS > 200) which were then combined using LogCombiner to obtain the final posterior distribution after removing 10% of each chain as burn-in. The results were analysed using the bdskytools package in R (https://github.com/laduplessis/bdskytools).

The resulting estimates for the time of the most recent common ancestor, exponential growth rate and doubling time are summarised in Extended Data Tables 4 and 5. With fixed clock rates of 0.75x10^{-3} and 1.1x10^{-3} s/s/y for the full South Africa and Botswana dataset and Gauteng Province only dataset, respectively, the 3-epoch and 4-epoch BDSKY models resulted in similar estimates of the effective reproduction number, R_e, for both datasets: 2.74 (95% HPD 2.56 - 2.92) and 2.79 (95% HPD 2.60 - 2.97) for the South Africa and Botswana dataset, and 3.86 (95% HPD 3.43 - 4.29) and 3.61 (95% HPD 3.20 - 4.02) for the Gauteng Province only dataset. Using a faster clock rate led to more recent common ancestors and higher estimates of the effective reproduction number and growth rate.

We explored the sensitivity of our estimates to different assumptions regarding the average duration of infectiousness by repeating the analysis of the South Africa and Botswana dataset with different fixed values of the becoming non-infectious rate: 52.1/year and 26.1/year which translates to an infectious period of 7 and 14 days, respectively. These values were selected as plausible bounds based on the infectious period of asymptomatic cases and the time from symptom onset to two negative RT-PCR tests[75]. The 4-epoch model was used with a fixed clock rate of 0.75x10^{-3} s/s/y in these analyses. For each analysis, we ran three independent chains of 35 million MCMC steps and sampled parameters every 10,000 steps. We used Tracer v1.7[76] to evaluate MCMC convergence for each of the individual chains (ESS > 200) which were then combined using LogCombiner to obtain the final posterior distribution after removing 10% of each chain as burn-in.

Results from the sensitivity analyses showed that our estimates are largely robust to alternative assumptions about the infectious period. On doubling of the mean duration of infectiousness from 7 to 14 days, the TMRCA remained mostly the same (10 October 2021 (95% HPD 2 October - 17 October) compared to 11 October 2021 (95% HPD 3 October - 17 October), while the doubling time shifted from 4.4 (95% HPD 3.9 - 5.0) days to 3.5 (95% HPD 3.2 - 3.9) days. This change in the doubling time is partially explained by differing estimates of the sampling proportion. For most of the epochs the sampling proportion increases with the doubling time in order to explain the same number of sequences observed in each instance, i.e. if we assume a shorter average duration of infectiousness, then we infer a slower transmission of which a greater proportion of sequences has been sampled.

Phylogeographic analysis. Markov Chain Monte Carlo (MCMC) analyses were run in duplicate in BEAST v1.10.4[70,71] for a total of 100 million iterations sampling every 10,000 steps in the chain. Convergence of runs was assessed in Tracer v1.7.1[76] based on high effective sample sizes (>200) and good mixing in the chains. Maximum clade credibility trees for each run were summarized in TreeAnnotator after discarding the first 10% of the chain as burn in. Finally, the spatiotemporal dispersal of Omicron was mapped using the R package "seraphim"[77].

Estimating transmission advantage. We analyzed 805 SARS-CoV-2 sequences from Gauteng, South Africa, that were uploaded to GISAID with sample collection dates from 1 September - 1 December 2021[15]. We used a multinomial logistic regression model to estimate the growth advantage of Omicron compared to Delta at the time point where the proportion of Omicron reached 50%[78,79]. We fitted the model using the *multinom* function of the *nnet* package and estimated the growth advantage using the package *emmeans* in R.

The difference in the net growth rates (i.e., the growth advantage) between a variant (Omicron) and the wild-type (Delta) can be expressed as follows[80]:

$$\rho = (1+\tau)\beta(S + \epsilon(1-S)) - \beta S,$$

where τ is the increase of the intrinsic transmissibility, ϵ is the level of immune evasion, β is the transmission rate of the wild-type, and S is the proportion of the population that is susceptible to the wild-type. This relation can be algebraically solved for τ and ϵ. We further define $R_w = \beta S D$ as the effective reproduction number of the wild-type with D being the generation time. $\Omega = 1 - S$ corresponds to the proportion of the population with protective immunity against infection and subsequent transmission with the wild-type.

We estimated ϵ for different levels of τ and Ω. To propagate the uncertainty, we constructed 95% credible intervals (CIs) of the estimates from 10,000 parameter samples of ρ, D, and R_w. We assumed D to be normally distributed with a mean of 5.2 days and a standard deviation of 0.8 days[81]. We sampled from publicly available estimates of the daily R_w based on confirmed cases during the early growth phase of Omicron

in South Africa (1 October - 31 October 2021; range: 0.78-0.85 (https://github.com/covid-19-Re)[82].

Reporting summary

Further information on research design is available in the Nature Research Reporting Summary linked to this paper.

Data availability

Code availability

49. Marivate, V. & Combrink, H. M. Use of Available Data To Inform The COVID-19 Outbreak in South Africa: A Case Study. *Data Sci. J.* **19**, (2020).
50. Marivate, V. et al. Coronavirus disease (COVID-19) case data - South Africa. *Zenodo* (2020) https://doi.org/10.5281/zenodo.3819126.
51. National Institute for Communicable Diseases. WEEKLY TESTING SUMMARY - NICD. https://www.nicd.ac.za/diseases-a-z-index/disease-index-covid-19/surveillance-reports/weekly-testing-summary/.
52. Wickham, H. ggplot2. *WIREs Comp Stat* **3**, 180–185 (2011).
53. Msomi, N., Mlisana, K., de Oliveira, T. & Network for Genomic Surveillance in South Africa writing group. A genomics network established to respond rapidly to public health threats in South Africa. *Lancet Microbe* **1**, e229–e230 (2020).
54. SARS-CoV2 genome sequencing protocol (1200bp amplicon "midnight" primer set, using Nanopore Rapid kit). https://doi.org/10.17504/protocols.io.bwyppfvn.
55. Cleemput, S. et al. Genome Detective Coronavirus Typing Tool for rapid identification and characterization of novel coronavirus genomes. *Bioinformatics* **36**, 3552–3555 (2020).
56. GitHub - epi2me-labs/wf-artic: ARTIC SARS-CoV-2 workflow and reporting. https://github.com/epi2me-labs/wf-artic#readme.
57. Bragg, L. M., Stone, G., Butler, M. K., Hugenholtz, P. & Tyson, G. W. Shining a light on dark sequencing: characterising errors in Ion Torrent PGM data. *PLoS Comput. Biol.* **9**, e1003031 (2013).
58. Robinson, J. T. et al. Integrative genomics viewer. *Nat. Biotechnol.* **29**, 24–26 (2011).
59. Hatcher, E. L. et al. Virus Variation Resource - improved response to emergent viral outbreaks. *Nucleic Acids Res.* **45**, D482–D490 (2017).
60. National Library of Medicine. NCBI Virus: SARS-CoV-2 Data Hub. https://www.ncbi.nlm.nih.gov/labs/virus/vssi/#/virus?SeqType_s=Nucleotide&VirusLineage_ss=SARS-CoV-2,%20taxid:2697049.
61. covid19-omicron-origins-recombination/aligned_234.shortnames.afa at main · bonilab/covid19-omicron-origins-recombination · GitHub. https://github.com/bonilab/covid19-omicron-origins-recombination/blob/main/4%20GS5%20plus%20Canada%20Outlier%20Lineage/4.2%20aligned_mafft_addfrag_wref/aligned_234.shortnames.afa.
62. Katoh, K., Misawa, K., Kuma, K. & Miyata, T. MAFFT: a novel method for rapid multiple sequence alignment based on fast Fourier transform. *Nucleic Acids Res.* **30**, 3059–3066 (2002).
63. Kosakovsky Pond, S. L. et al. HyPhy 2.5-A Customizable Platform for Evolutionary Hypothesis Testing Using Phylogenies. *Mol. Biol. Evol.* **37**, 295–299 (2020).
64. Benton, D. J. et al. Receptor binding and priming of the spike protein of SARS-CoV-2 for membrane fusion. *Nature* **588**, 327–330 (2020).
65. Aksamentov, I., Roemer, C., Hodcroft, E. & Neher, R. Nextclade: clade assignment, mutation calling and quality control for viral genomes. *JOSS* **6**, 3773 (2021).
66. Price, M. N., Dehal, P. S. & Arkin, A. P. FastTree 2 — approximately maximum-likelihood trees for large alignments. *PLoS ONE* **5**, e9490 (2010).
67. Felsenstein, J. Confidence limits on phylogenies: an approach using the bootstrap. *Evolution* **39**, 783–791 (1985).
68. Sagulenko, P., Puller, V. & Neher, R. A. TreeTime: Maximum-likelihood phylodynamic analysis. *Virus Evol.* **4**, vex042 (2018).
69. Yu, G. Using ggtree to Visualize Data on Tree-Like Structures. *Curr. Protoc. Bioinformatics* **69**, e96 (2020).
70. Suchard, M. A. et al. Bayesian phylogenetic and phylodynamic data integration using BEAST 1.10. *Virus Evol.* **4**, vey016 (2018).
71. Drummond, A. J., Suchard, M. A., Xie, D. & Rambaut, A. Bayesian phylogenetics with BEAUti and the BEAST 1.7. *Mol. Biol. Evol.* **29**, 1969–1973 (2012).
73. Bouckaert, R. et al. BEAST 2.5: An advanced software platform for Bayesian evolutionary analysis. *PLoS Comput. Biol.* **15**, e1006650 (2019).
74. Benvenuto, D. et al. The global spread of 2019-nCoV: a molecular evolutionary analysis. *Pathog. Glob. Health* **114**, 64–67 (2020).
75. Byrne, A. W. et al. Inferred duration of infectious period of SARS-CoV-2: rapid scoping review and analysis of available evidence for asymptomatic and symptomatic COVID-19 cases. *BMJ Open* **10**, e039856 (2020).
76. Rambaut, A., Drummond, A. J., Xie, D., Baele, G. & Suchard, M. A. Posterior summarization in Bayesian phylogenetics using tracer 1.7. *Syst. Biol.* **67**, 901–904 (2018).
77. Dellicour, S., Rose, R., Faria, N. R., Lemey, P. & Pybus, O. G. SERAPHIM: studying environmental rasters and phylogenetically informed movements. *Bioinformatics* **32**, 3204–3206 (2016).
78. Davies, N. G. et al. Estimated transmissibility and impact of SARS-CoV-2 lineage B.1.1.7 in England. *Science* **372**, (2021).
79. Campbell, F. et al. Increased transmissibility and global spread of SARS-CoV-2 variants of concern as at June 2021. *Euro Surveill.* **26**, (2021).
80. Althaus, C. L. et al. A tale of two variants: Spread of SARS-CoV-2 variants Alpha in Geneva, Switzerland, and Beta in South Africa. *medRxiv* (2021) https://doi.org/10.1101/2021.06.10.21258468.
81. Ganyani, T. et al. Estimating the generation interval for coronavirus disease (COVID-19) based on symptom onset data, March 2020. *Euro Surveill.* **25**, (2020).
82. Huisman, J. S. et al. Estimation and worldwide monitoring of the effective reproductive number of SARS-CoV-2. *medRxiv* (2020) https://doi.org/10.1101/2020.11.26.20239368.
83. Stamatakis, A. RAxML version 8: a tool for phylogenetic analysis and post-analysis of large phylogenies. *Bioinformatics* **30**, 1312–1313 (2014).
84. Boni, M. F. et al. Evolutionary origins of the SARS-CoV-2 sarbecovirus lineage responsible for the COVID-19 pandemic. *Nat. Microbiol.* **5**, 1408–1417 (2020).

Article

Extended Data Fig. 1 | Progression of daily recorded cases and variant proportions in Gauteng (A), KwaZulu-Natal (B) and Western Cape (C) provinces between October and December 2021. A sharp increase in the 7-day rolling average of the number of cases is observed in all three of the biggest provinces in South Africa at the emergence of the Omicron variant.
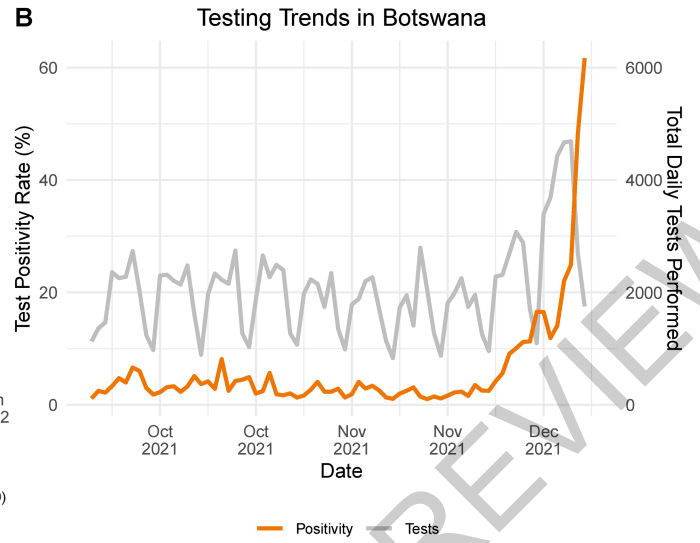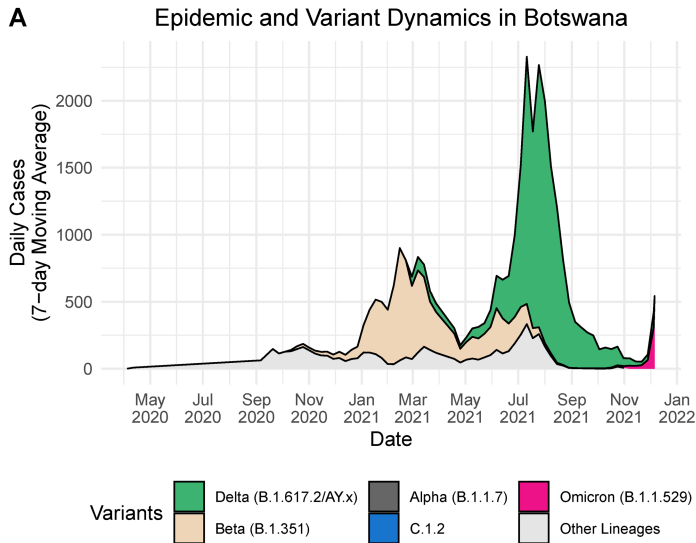
A Epidemic and Variant Dynamics in Botswana

B Testing Trends in Botswana

Variants: Delta (B.1.617.2/AY.x), Beta (B.1.351), Alpha (B.1.1.7), C.1.2, Omicron (B.1.1.529), Other Lineages

Positivity, Tests

Extended Data Fig. 2 | Epidemic Progression in Botswana. A) Epidemic and variant dynamics in Botswana from May 2020 to December 2021, with the 7-day rolling average of the number of recorded cases coloured by the proportion of variants as inferred by genomic surveillance data available on GISAID. At the end of November 2021, a big Delta-driven wave was coming to its end and an Omicron wave was starting at the end of November 2021. B) Trends in testing numbers and positivity rates in Botswana between October and December 2021, showing a sharp increase in positivity rate mid-November 2021.

Article

Extended Data Fig. 3 | Global distribution of Omicron. (A) Detection of Omicron globally. Shown are the locations for which Omicron genomes have been deposited on GISAID as of December 16, 2021. Those labelled as "reported" referred to the country from which Omicron has been reported to the WHO but there is currently no sequencing data available in GISAID, all data comes from GISAID and the WHO weekly epidemiology report Edition 70 dated December 14, 2021 (https://reliefweb.int/sites/reliefweb.int/files/resources/20211207_Weekly_Epi_Update_69-%281%29.pdf). Countries are coloured according to the number of genomes deposited with warmer colours representing more genomes. (B) Omicron transmission globally. Shown are countries for which Omicron sequencing data is available on GISAID. Proportions of sequences are coloured according to sampling strategy or additional host/location information from either travel history, targeted sequencing (specifically for SGTF, vaccine breakthroughs, outbreaks, contact tracing or other reasons), routine surveillance or unknown if no information has been provided. Countries are ordered by the number of sequences available on GISAID as of December 16, 2021.

A BA.2

S1 Subunit | S2 Subunit

13 | 303 | 319 | 541 | Furin cleavage site 680 744

NTD | RBD | SD1/SD2

1 | 250 | 750 | 1000 | 1250

T19I
L24S
Δ25-27
G142D
V213G
G339D
S371F
S373P
S375F
T376A
D405N
R408S
K417N
N440K
G446S
Q493K
E484A
T478K
S477N
Q498R
Y505H
N501Y
T547K
P681H
N679K
H655Y
D614G
D796Y
N764K
Q954H
N969K

B BA.3

S1 Subunit | S2 Subunit

13 | 303 | 319 | 541 | Furin cleavage site 680 744

NTD | RBD | SD1/SD2

1 | 250 | 750 | 1000 | 1250

A67V
Δ69-70
T95I
G142D
R214
Insertion 211
Δ211
Δ143-145
L212I
G339D
S371F
S373P
S375F
D405N
K417N
N440K
G446S
N501Y
Y505H
Q498R
Q493K
E484A
T478K
S477N
P681H
N679K
H655Y
D614G
D796Y
N764K
Q954H
N969K

C

Omicron

D

BA.1

BA.2

BA.3

Extended Data Fig. 4 | Related Lineages BA.2 and BA.3 Molecular Profile and Evolutionary Origins. A) Amino-acid mutations on the spike gene of the BA.2 B) Amino-acid mutations on the spike gene of the BA.3 C) Raw maximum likelihood phylogeny of 13,462 SARS-CoV-2 genomes, including 148 BA.2 and

19 BA.3. The newly identified SARS-CoV-2 Omicron variant is shown in colour versus grey for all other lineages. **D**) A zoomed-in view of the Omicron clade showing the evolutionary relationship between BA.1, BA.2 and BA.3.
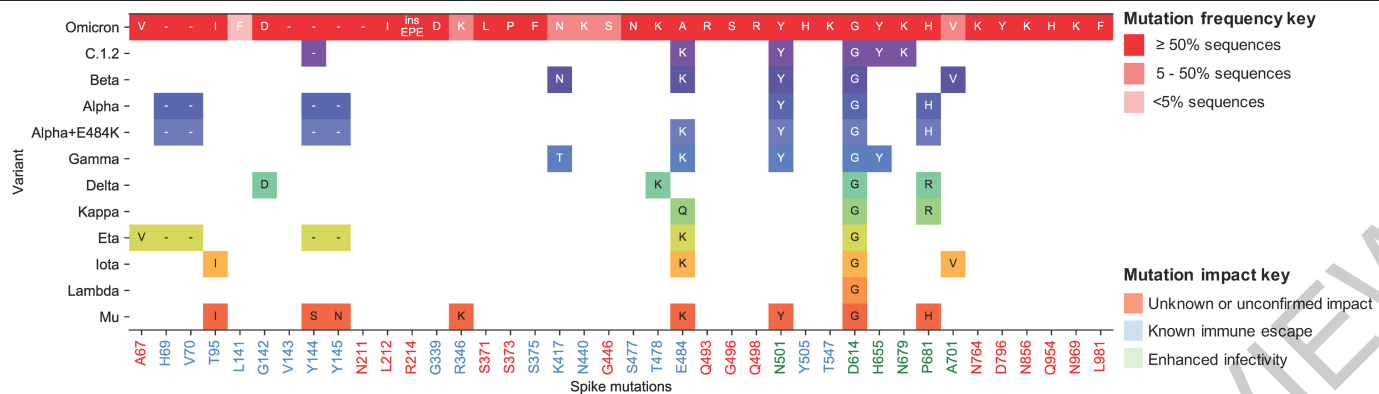
Extended Data Fig. 5 | Omicron/BA.1 spike mutations shared with other VOC/VOIs. All spike mutations seen in Omicron/BA.1 are listed at the top in red and coloured according to prevalence. Prevalence was calculated by number of mutation detections / total number of sequences. However, primer drop-outs have affected the RBD region spanning K417N, N440K and G446S, and so it is likely that these mutations may actually be more prevalent than indicated here. For the VOC/VOIs only mutations that are shared with Omicron and seen in ≥50% of the respective VOC/VOI sequences are shown and are coloured according to Nextstrain clade. The mutations listed at the bottom are shaded according to known immune escape (blue), enhanced infectivity (green) or for unknown/unconfirmed impact (red).

Region 1: positions 1 - 21690
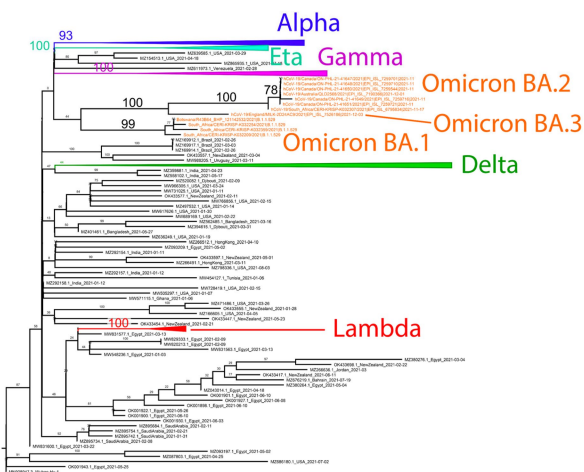
Region 2: positions 21691 - 22587

Region 3: positions 22588 - 30012

Extended Data Fig. 6 | Maximum-likelihood trees (inferred with RAxML v8.2.12[83]) for genome regions bounding the consensus recombination breakpo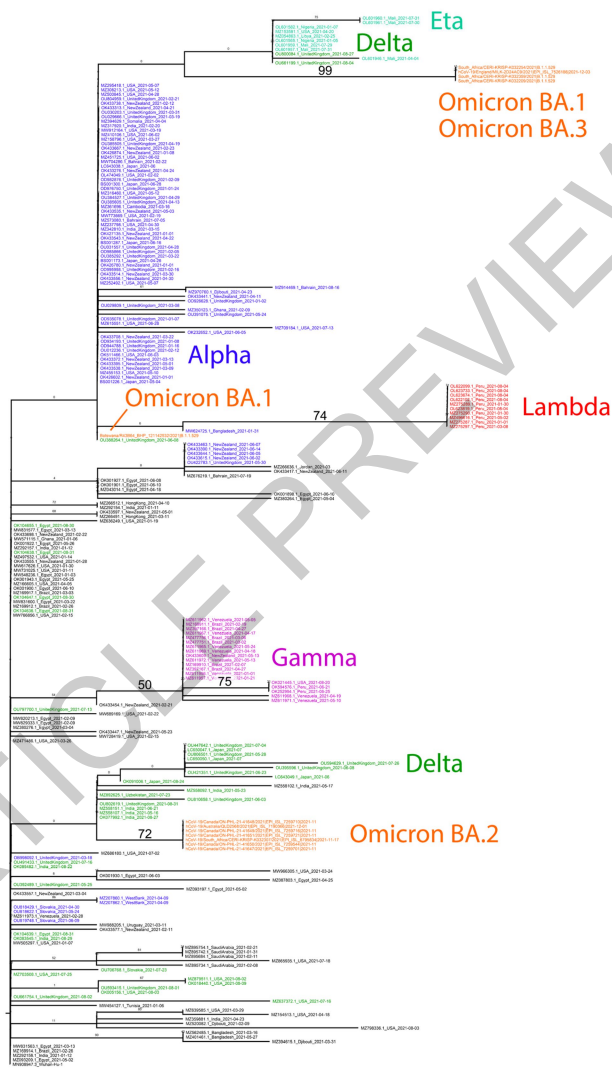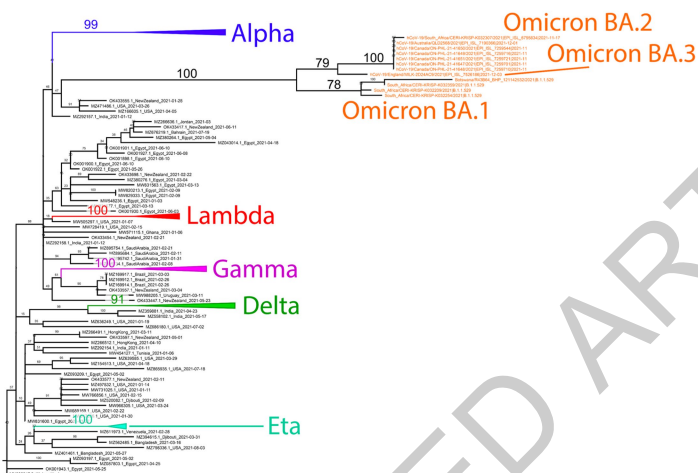ints detected in lineages BA.1, BA.2 and BA.3[84]. The trees include SARS-CoV-2 genome sequences sampled in 2021 (N=221) together with 13 sequences representing the BA.1/Omicron, BA.2 and BA.3 lineages. Whereas in trees for regions 1 and 3 BA.2 and BA.3 cluster together with high bootstrap support, BA.1 is a well-supported albeit more distantly related sibling lineage. The a 897nt region 2 segment (encoding the N-terminal domain of Spike) includes 67 polymorphic sites with a maximum 8nt difference between strains, showing little bootstrap support for any sibling or clade relationships except the membership of certain viruses in WHO-designated clades (Lambda, Omicron, Gamma). Despite Omicron lineages BA.1 and BA.3 clustering with certain Delta and Eta viruses and Omicron BA.2 clustering with a distinct set of Delta viruses (all on the basis of several key nucleotide positions), trees based on region 2 show no statistical support for the three Omicron lineages having distinct evolutionary origins. Bootstrap values are shown on branches with relevant values magnified for readability. All trees were rooted on the Wuhan-Hu-1 sequence.

Article

Extended Data Table 1 | Parameter estimates from BEAST for the full South Africa and Botswana dataset and the reduced data set of only Gauteng Province genomes

Data set	Evolutionary rate x10^{-3} changes/site/year	BA.1 Time of most recent common ancestor (TMRCA)	Exponential growth rate (per day)	Doubling time (days)
South Africa + Botswana 553 Genomes	1.20 (0.92, 1.49)	9 Oct 2021 (30 Sep, 20 Oct)	0.137 (0.099, 0.175)	5.1 (4.0, 7.0)
South Africa + Botswana 553 Genomes	1.1 fixed	8 Oct 2021 (30 Sep, 18 Oct)	0.137 (0.100, 0.173)	5.0 (4.0, 7.0)
South Africa + Botswana 553 Genomes	0.75 fixed	1 Oct 2021 (21 Sep, 13 Oct)	0.139 (0.099, 0.183)	5.0 (3.8, 7.0)
Gauteng Province, South Africa only 626 genomes 2021-11-05, 2021-12-07	0.41 (0.28, 0.54)	01 Oct 2021 (17 Sept, 17 Oct)	2.85 (2.10, 4.23)	2.8 (2.1, 4.2)
Gauteng Province, South Africa only 626 genomes 2021-11-05, 2021-12-07	1.1 fixed	19 Oct 2021 (15 Oct, 26 Oct)	0.29 (0.22, 0.35)	2.42 (1.96, 3.12)

95% Highest Posterior Density (HPD) intervals in parentheses.

Extended Data Table 2 | Sites in the Omicron/BA.1 sequences that have been subject to episodic diversifying selection

Coordinate (SARS-CoV-2)	Gene/ORF	Codon (in gene/ORF)	# of selected branches	AA composition	p-value	Notes
3682	ORF1a	1140	1	Q/92, L/2	0.0061	
13423	ORF1a	4387	2	R/34, H/1, N/1	0.0020	
13627	ORF1b	54	1	D/256, -/2, Y/1	0.0098	
18027	ORF1b	1520	1	A/171, -/12, Y/1, V/1	0.0006	
18030	ORF1b	1521	2	T/171, -/12, K/1, I/1	0.0052	
18267	ORF1b	1600	1	E/184, T/1, -/1	0.0001	
18273	ORF1b	1602	1	A/184, C/1, -/1	0.0001	
21534	ORF1b	2689	1	D/85, S/3	0.0066	
22027	S	156	3	E/172, -/11, G/5, P/1	0.0006	
22033	S	158	1	R/165, -/23, S/1	0.0007	
22048	S	163	1	A/168, -/20, L/1	0.0036	
22072	S	171	2	V/167, -/21, K/1	0.0000	
22084	S	175	1	F/161, -/26, Q/2	0.0000	
22576	S	339	3	D/170, -/11, G/8	0.0027	Clade defining
22597	S	346	5	R/151, K/32, -/6	0.0007	Affect Ab binding
22672	S	371	1	L/154, S/18, -/16, F/1	0.0002	Clade defining
22678	S	373	4	P/149, S/26, -/14	0.0009	Clade defining
22684	S	375	5	F/142, S/34, -/13	0.0001	Clade defining
22810	S	417	5	N/113, K/41, -/35	0.0002	Clade defining
22879	S	440	4	K/120, -/36, N/33	0.0018	Clade defining
22897	S	446	5	S/124, -/38, G/27	0.0002	Clade defining
22915	S	452	4	L/138, -/36, R/15	0.0000	Affect Ab binding
22990	S	477	3	N/148, -/23, S/18	0.0005	Clade defining
23011	S	484	3	A/141, -/26, E/21, V/1	0.0016	Clade defining
23047	S	496	3	S/151, G/21, -/17	0.0051	Clade defining
23053	S	498	2	R/148, -/21, Q/20	0.0028	Clade defining
23074	S	505	4	H/142, Y/25, -/22	0.0002	Clade defining
23095	S	512	1	V/170, -/18, T/1	0.0008	
23662	S	701	3	A/156, V/25, -/7, S/1	0.0034	501Y metasignature
23851	S	764	0	K/150, N/23, -/15, H/1	0.0010	Clade defining
24502	S	981	3	F/180, L/6, -/3	0.0084	Clade defining
25548	ORF3a	53	1	L/178, F/2	0.0099	
25707	ORF3a	106	1	L/158, F/22	0.0072	
26528	M	3	2	G/113, -/26, D/9, Y/1	0.0041	
26708	M	63	3	T/110, -/28, A/11	0.0016	Clade defining
26765	M	82	3	I/111, -/28, T/10	0.0019	
27140	M	207	1	N/105, -/42, R/1, S/1	0.0011	
27143	M	208	2	T/104, -/42, S/2, I/1	0.0066	
27146	M	209	1	D/104, -/42, A/2, Y/1	0.0008	
28253	ORF8	121	3	F/271, I/162, -/24, L/10, V/6, K/5, S/4, Q/1, D/1, C/1	0.0013	
28459	N	63	2	D/272, G/11, -/11, Y/1	0.0010	
28471	N	67	2	P/280, -/11, S/3, L/1	0.0070	
28477	N	69	1	G/282, -/11, K/2	0.0001	
28879	N	203	3	K/283, M/8, I/2, -/1, R/1	0.0088	Clade defining
29299	N	343	3	D/253, G/40, C/1, H/1	0.0002	

Article

Extended Data Table 3 | Prior distributions used for the BDSKY analyses

Parameter	Prior distribution	
	South Africa and Botswana (n = 552)	Gauteng Province only (n = 277)
clock rate (x10^{-3} substitutions/site/year)	0.75 fixed; 1.2 fixed	1.1 fixed; 0.3 fixed
kappa	Lognormal(lnMean = 1, lnSd = 1.25)	
gamma shape	Exponential(m = 1)	
effective reproduction number	Lognormal(lnMean = 0.8, lnSd = 0.5)	
becoming non-infectious rate (per year)	36.5 fixed	
sampling proportion	Beta(alpha = 2, beta = 1000)	Beta(alpha = 2, beta = 100)
time of origin	Lognormal(lnMean = -2, lnSd = 0.2)	

The becoming non-infectious rate was fixed to 36.5/year which corresponds to a mean infectious period of 10 days. A less informative prior for the sampling proportion was used for the Gauteng Province only dataset to allow for the possibility of a higher province-specific sampling proportion.

Extended Data Table 4 | Time of most recent common ancestor, exponential growth rate and doubling time estimates for the full South Africa and Botswana dataset and the reduced dataset of only Gauteng Province genomes under the 3-epoch BDSKY model in which the sampling proportion was allowed to change at 3 equidistantly spaced time points

	Fixed clock rate ($\times 10^{-3}$ substitutions/site/year)	Time of most recent common ancestor (TMRCA)	Exponential growth rate (per day)	Doubling time (days)
South Africa and Botswana (n = 522)	1.20	20 Oct 2021 (13 Oct, 26 Oct)	0.206 (0.188, 0.226)	3.4 (3.0, 3.7)
	0.75	11 Oct 2021 (3 Oct, 18 Oct)	0.174 (0.156, 0.192)	4.0 (3.6, 4.4)
Gauteng Province only (n = 277)	0.30	4 Oct 2021 (24 Sep, 12 Oct)	0.191 (0.151, 0.231)	3.6 (2.9, 4.5)
	1.1	24 Oct 2021 (19 Oct, 29 Oct)	0.286 (0.243, 0.329)	2.4 (2.1, 2.8)

95% Highest Posterior Density (HPD) intervals in parentheses.

Extended Data Table 5 | Time of most recent common ancestor, exponential growth rate and doubling time estimates for the full South Africa and Botswana dataset and the reduced dataset of only Gauteng Province genomes under the 4-epoch BDSKY model in which the sampling proportion was allowed to change at 4 equidistantly spaced time points

	Fixed clock rate (x10⁻³ substitutions/site/year)	Time of most recent common ancestor (TMRCA)	Exponential growth rate (per day)	Doubling time (days)
South Africa and Botswana (n = 522)	1.20	19 Oct 2021 (13 Oct, 25 Oct)	0.205 (0.186, 0.225)	3.4 (3.1, 3.7)
	0.75	11 Oct 2021 (2 Oct, 17 Oct)	0.179 (0.160, 0.197)	3.9 (3.5, 4.3)
Gauteng Province only (n = 277)	0.30	27 Sep 2021 (16 Sep, 7 Oct)	0.146 (0.114, 0.180)	4.8 (3.8, 5.9)
	1.1	23 Oct 2021 (17 Oct, 28 Oct)	0.261 (0.220, 0.302)	2.7 (2.3, 3.1)

95% Highest Posterior Density (HPD) intervals in parentheses.

nature research

Corresponding author(s):	Tulio de Oliveira
Last updated by author(s):	Jan 6, 2022

Reporting Summary

Nature Research wishes to improve the reproducibility of the work that we publish. This form provides structure for consistency and transparency in reporting. For further information on Nature Research policies, see Authors & Referees and the Editorial Policy Checklist.

Statistics

For all statistical analyses, confirm that the following items are present in the figure legend, table legend, main text, or Methods section.

n/a	Confirmed	
☐	☒	The exact sample size (*n*) for each experimental group/condition, given as a discrete number and unit of measurement
☐	☒	A statement on whether measurements were taken from distinct samples or whether the same sample was measured repeatedly
☐	☒	The statistical test(s) used AND whether they are one- or two-sided *Only common tests should be described solely by name; describe more complex techniques in the Methods section.*
☒	☐	A description of all covariates tested
☐	☒	A description of any assumptions or corrections, such as tests of normality and adjustment for multiple comparisons
☐	☒	A full description of the statistical parameters including central tendency (e.g. means) or other basic estimates (e.g. regression coefficient) AND variation (e.g. standard deviation) or associated estimates of uncertainty (e.g. confidence intervals)
☐	☒	For null hypothesis testing, the test statistic (e.g. *F*, *t*, *r*) with confidence intervals, effect sizes, degrees of freedom and *P* value noted *Give P values as exact values whenever suitable.*
☐	☒	For Bayesian analysis, information on the choice of priors and Markov chain Monte Carlo settings
☐	☒	For hierarchical and complex designs, identification of the appropriate level for tests and full reporting of outcomes
☒	☐	Estimates of effect sizes (e.g. Cohen's *d*, Pearson's *r*), indicating how they were calculated

Our web collection on statistics for biologists contains articles on many of the points above.

Software and code

Policy information about availability of computer code

Data collection	No software was used
Data analysis	Base-calling for GridIon sequencing was performed on MinKNOW software v21.6. Genome assembly was performed with Genome Detective online tool version 1.132 or Exatype NGS SARS-CoV-2 pipeline v1.6.1 or SARSCoV2 RECoVERY (REconstruction of COronaVirus gEnomes & Rapid analYsis) pipeline implemented in the Galaxy instance ARIES (https://aries.iss.it) and validated with Geneious software v.2020.1.2, IG Viewer or Aliview v1.27. Phylogenetic analysis was performed using FastTree2.1, MAFFT v7.490, Nextalign, BEASTv.1.10.4, BEAST2 v2.5.2, and Tracer v.1.7.1. Selection analyses were performed using HyPhy v2.5.33 through the RASCL pipeline. Recombination analyses were performed using 3SEQ, RDP5 and GARD. Lineage classification was performed using the PANGO software suite (lineages v1.2.106). Structure modeling visualization was performed using PyMOL Molecular Graphics System, version 2.2.0. R packages used for data analysis included ggplot, ggtree, seraphim. Custom codes are all available at: https://github.com/krisp-kwazulu-natal/ SARSCoV2_Omicron_Southern_Africa.

For manuscripts utilizing custom algorithms or software that are central to the research but not yet described in published literature, software must be made available to editors/reviewers. We strongly encourage code deposition in a community repository (e.g. GitHub). See the Nature Research guidelines for submitting code & software for further information.

Data

Policy information about availability of data

All manuscripts must include a data availability statement. This statement should provide the following information, where applicable:

- Accession codes, unique identifiers, or web links for publicly available datasets
- A list of figures that have associated raw data
- A description of any restrictions on data availability

Data availability Statement: All SARS-CoV-2 whole genome sequences produced by NGS-SA are deposited in the GISAID sequence database and are publicly available subject to the terms and conditions of the GISAID database. The GISAID accession numbers of sequences used in the phylogenetic analysis, including

Field-specific reporting

Please select the one below that is the best fit for your research. If you are not sure, read the appropriate sections before making your selection.

☒ Life sciences ☐ Behavioural & social sciences ☐ Ecological, evolutionary & environmental sciences

For a reference copy of the document with all sections, see nature.com/documents/nr-reporting-summary-flat.pdf

Life sciences study design

All studies must disclose on these points even when the disclosure is negative.

Sample size	No sample size calculation was performed; rather all genomic data available at the time of writing for the newly emerged Omicron variant was considered to ensure most accurate analysis and results in a timely manner. At the time of writing (11 December 2021), 553 good quality sequences of the Omicron SARS-CoV-2 variant had been produced by the NGS-SA and Botswana Harvard HIV Reference Laboratory (BHHRL) in South Africa (all fastq in SRA). We believe this was a sufficient sample size as the genomes spanned 8 of the 9 provinces of South Africa, including from multiple districts and two regions of Botswana. For phyloegentic analysis, this was analyzed against a globally representative reference set of SARS-CoV-2 genotypes (n=12 609) spanning the entire genetic diversity observed since the start of the pandemic.
Data exclusions	For phylogenetic analysis and time-calibrated BEAST analysis, genomes were excluded if they presented <90% coverage against the reference AND/OR have sequencing quality problem - e.g. gaps in key regions of the spike protein that causes spurious clustering.
Replication	Reproducibility were performed for maximum likelihood (bootstrap x1000 with FastTree) and bayesian MCMC phylogenetic tree reconstructions. We computed MCMC (Markov chain Monte Carlo) triplicate runs of 100 million states each, sampling every 10,000 steps for the Omicron dataset. All attempts at replication were successful and the MCC tree for the Omicron cluster was of high support.
Randomization	Experimental groups consisted of weekly batches of residual patient nasopharyngeal swabs selected for sequencing to determine the progression of weekly lineage prevalence as part of surveillance. Samples for weekly SARS-CoV-2 sequencing in South Africa and Botswana were selected at random from all relevant divisions in each country, without any clinical or geographical bias. Generally, part of the Network for Genomic Surveillance in South Africa (NGS-SA), five sequencing hubs receive randomly selected samples for sequencing every week according to approved protocols at each site. In response to a rapid resurgence of COVID-19 in Gauteng Province in November, we enriched our routine sampling with additional samples from those areas.
Blinding	Geographical blinding of data was not necessary for the study as it involves phylogeographical analysis. Other types of blinding were also not necessary as this was not a cohort study.

Reporting for specific materials, systems and methods

We require information from authors about some types of materials, experimental systems and methods used in many studies. Here, indicate whether each material, system or method listed is relevant to your study. If you are not sure if a list item applies to your research, read the appropriate section before selecting a response.

Materials & experimental systems

n/a	Involved in the study
☒	☐ Antibodies
☒	☐ Eukaryotic cell lines
☒	☐ Palaeontology
☒	☐ Animals and other organisms
☐	☒ Human research participants
☒	☐ Clinical data

Methods

n/a	Involved in the study
☒	☐ ChIP-seq
☒	☐ Flow cytometry
☒	☐ MRI-based neuroimaging

Human research participants

Policy information about studies involving human research participants

Population characteristics	We obtained samples consisting of remnant nucleic acid extracts or remnant nasopharyngeal and oropharyngeal swab samples from routine diagnostic SARS-CoV-2 PCR testing from public and private laboratories in South Africa. The Omicron genomes in

this study came from patients of ages 0-82, with an approximately equal distribution of males and females, for which the Omicron genotype was confirmed by sequencing.

Recruitment

As part of the Network for Genomic Surveillance in South Africa (NGS-SA), five sequencing hubs receive randomly selected samples for sequencing every week according to approved protocols at each site. In response to a rapid resurgence of COVID-19 in the province of Gauteng in November, we enriched our routine sampling with additional samples from this area. One bias that may be present is the ability to sequence only from the pool of patients that seek testing and that receive a positive PCR test.

Ethics oversight

The genomic surveillance in South Africa was approved by the University of KwaZulu–Natal Biomedical Research Ethics Committee (BREC/00001510/2020), the University of the Witwatersrand Human Research Ethics Committee (HREC) (M180832), Stellenbosch University HREC (N20/04/008_COVID-19), University of Cape Town HREC (383/2020), University of Pretoria HREC (H101/17) and the University of the Free State Health Sciences Research Ethics Committee (UFS-HSD2020/1860/2710). The genomic sequencing in Botswana was conducted as part of the national vaccine roll-out plan and was approved by the Health Research and Development Committee (Health Research Ethics body, HRDC#00948 and HRDC#00904). Individual participant consent was not required for the genomic surveillance. This requirement was waived by the Research Ethics Committees.

Note that full information on the approval of the study protocol must also be provided in the manuscript.